

台灣西南部麓山帶之構造

中央大學地球科學系

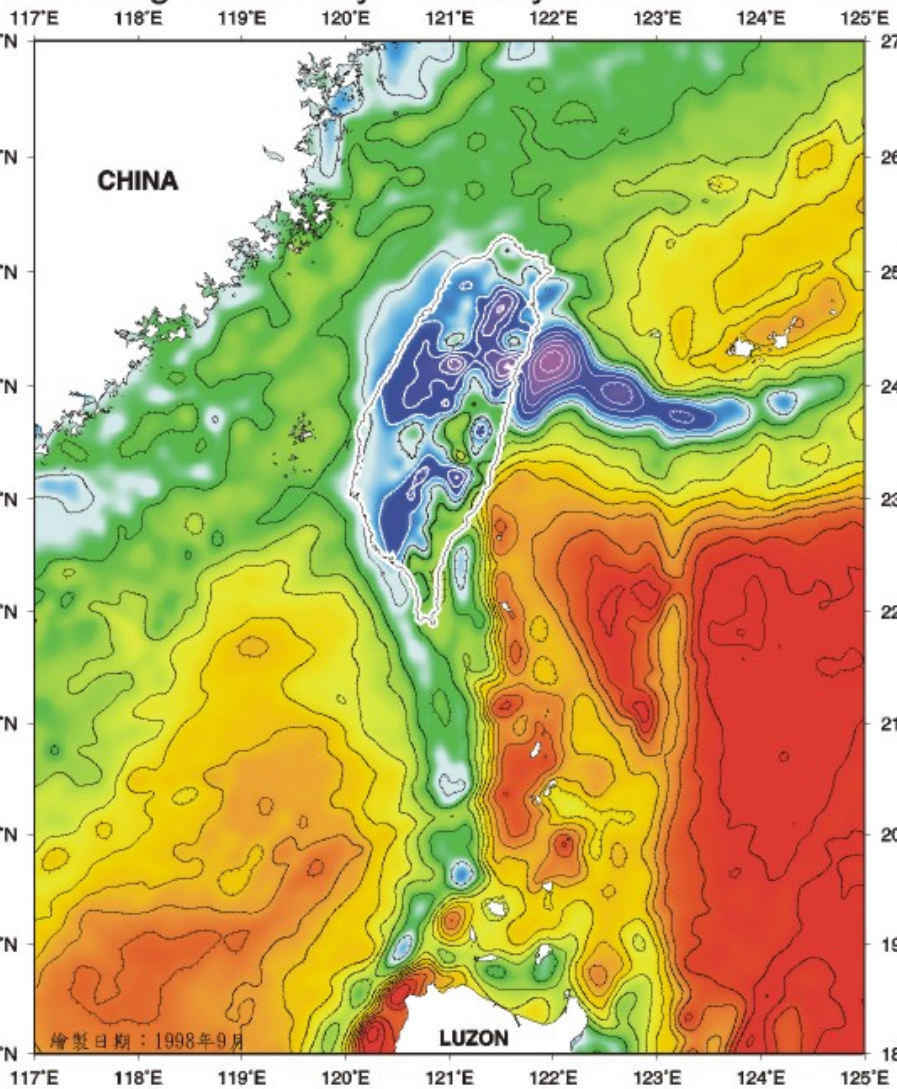
洪日豪

- 薄皮與厚皮構造的造山模式對地下構造的解釋
 - 基底滑脫面的存在與否
 - 基底滑脫面的深度與形貌
- 地下構造與地震資料的結合
- 西部麓山帶之構造型式
- 正斷層重新活動的模式與力學機制
- 新構造運動
 - 長期（地質時間）VS 短期（大地測量）滑移速率
 - 地震規模的估算
 - 構造與地形演化

Geodynamic models of Taiwan

- Mode of Crustal Deformation
 - Decollement, Escape
- Crustal-Upple mantle coupling
- Delamination
- Subduction – continental or lost slab
- Upper mantle flow
- Collision
- Intraplate deformation
- Thin-skinned -- Suppe
- Thin-skinned with subduction – Lellamand, Malaville
- Lithospheric thickening - Wu

台灣周圍布蓋重力異常圖
Bouguer Gravity Anomaly around Taiwan



Bouguer gravity anomaly (mGal)



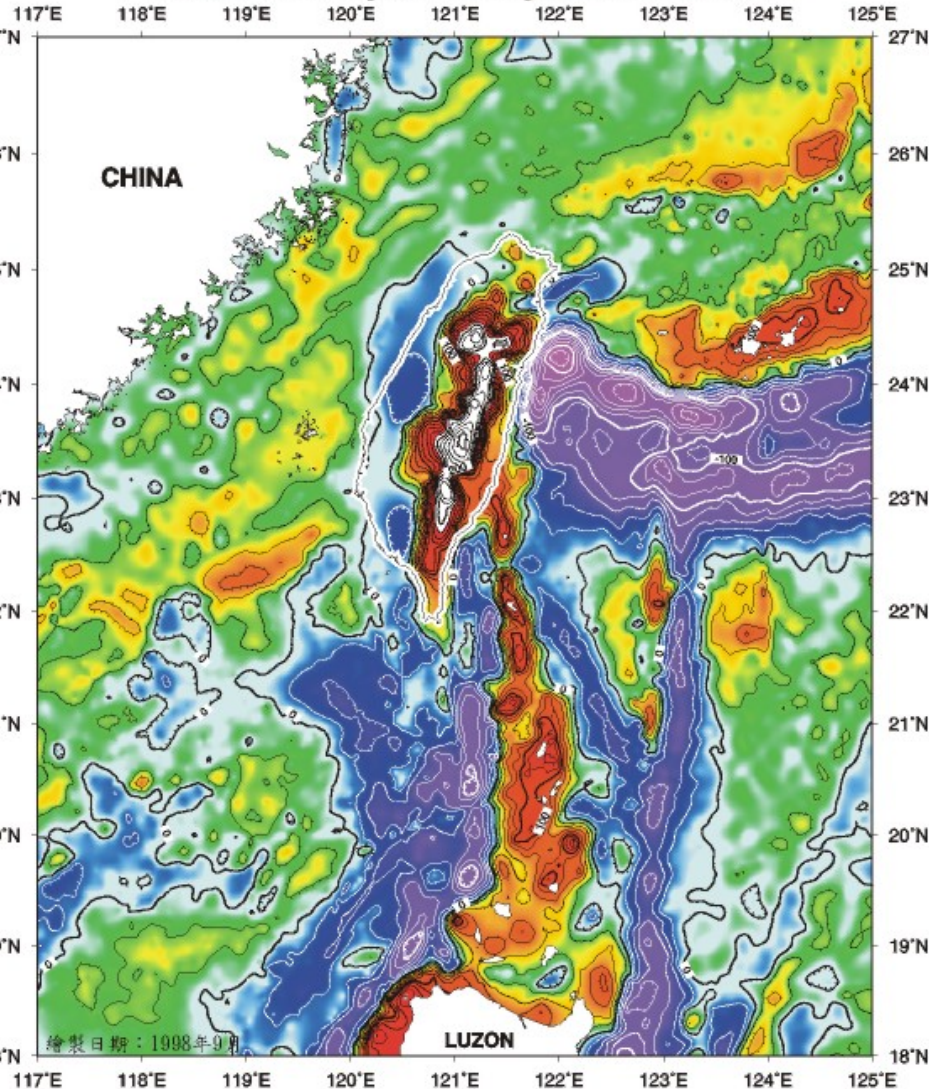
編製單位：
 國立台灣大學海洋研究所
 國家海洋科學研究中心海洋資料庫

資料來源及整編請參考：

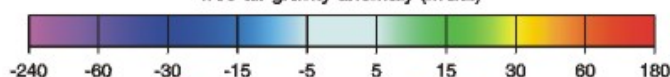
Hsu, S. K., C. S. Liu, C. T. Shyu, S. Y. Liu, J. C. Sibuet, S. Lallemand, C. Wang, and D. Reed, 1998: New gravity and magnetic anomaly maps in the Taiwan-Luzon region and their preliminary interpretation., TAO, Vol. 9, No. 3, 509-532.

ODB CD003: gravity/hsu bq 1am.ard

台灣周圍自由空間重力異常圖
Free-Air Gravity Anomaly around Taiwan



free-air gravity anomaly (mGal)

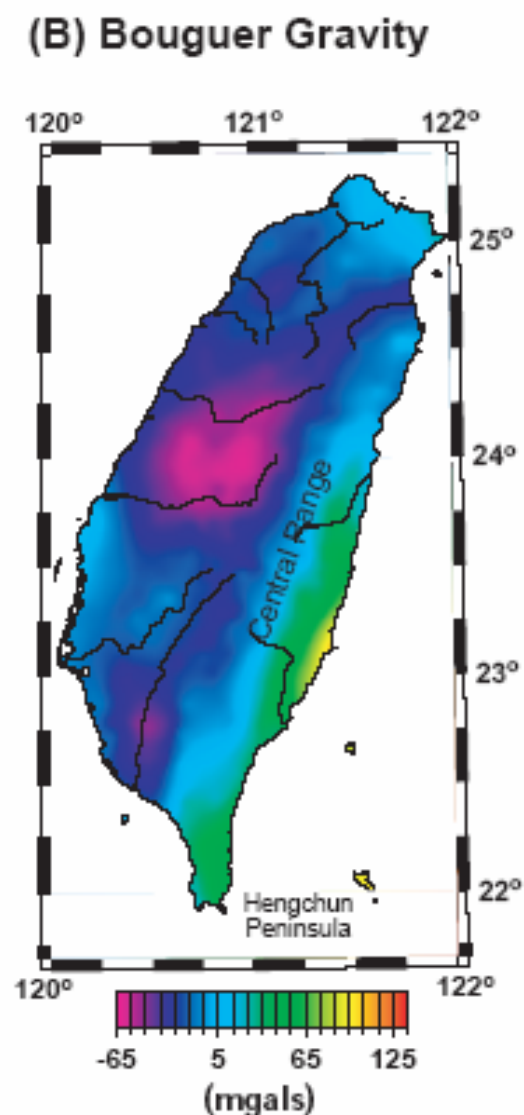
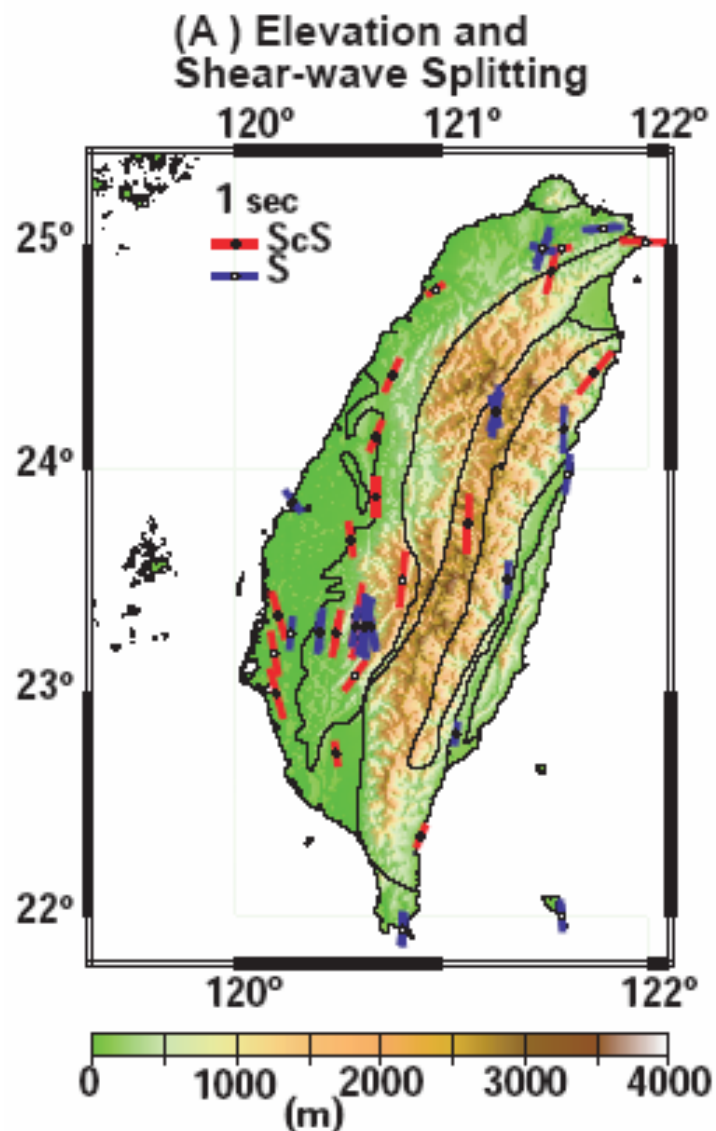


編製單位：
 國立台灣大學海洋研究所
 國家海洋科學研究中心海洋資料庫

資料來源及整編請參考：

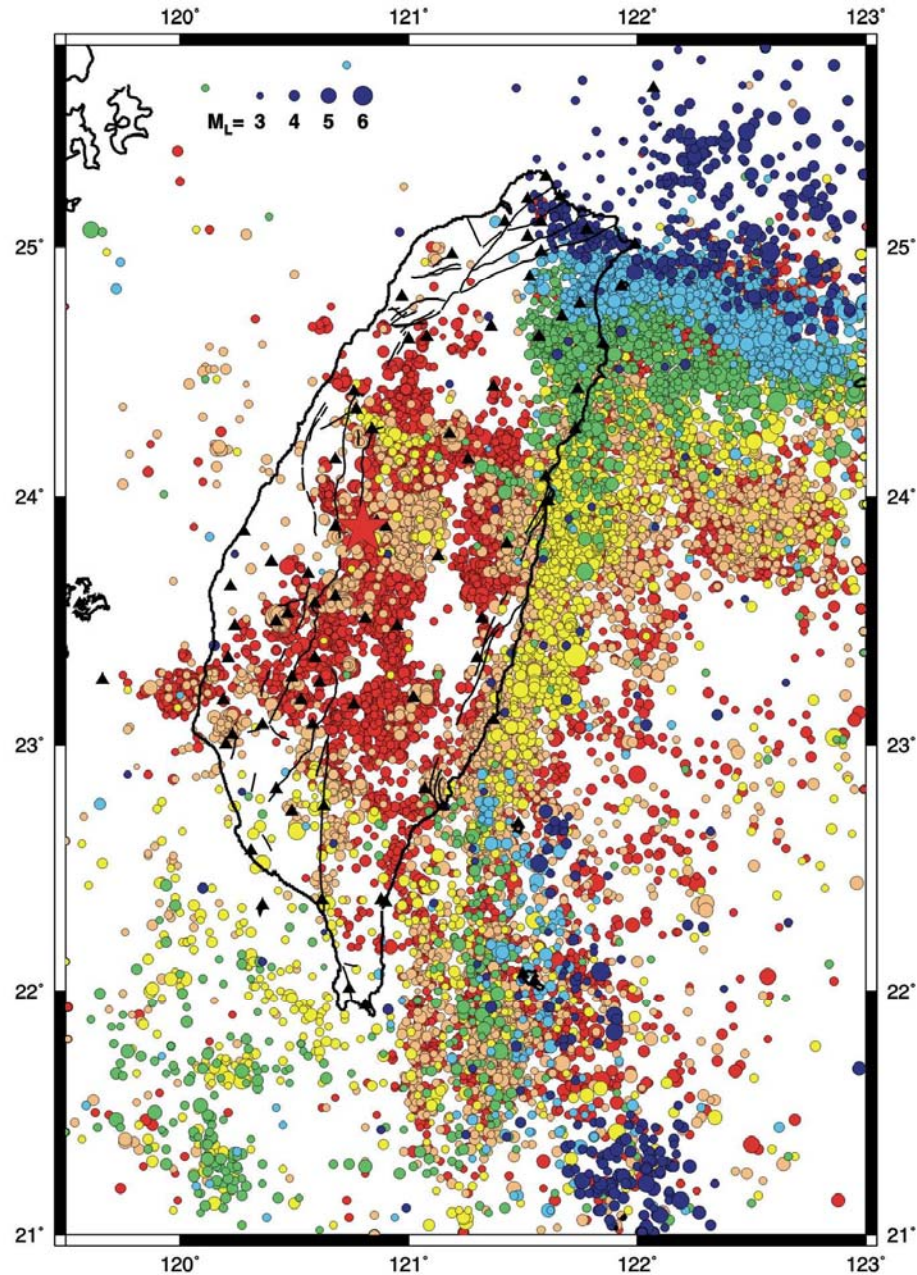
Hsu, S. K., C. S. Liu, C. T. Shyu, S. Y. Liu, J. C. Sibuet, S. Lallemand, C. Wang, and D. Reed, 1998: New gravity and magnetic anomaly maps in the Taiwan-Luzon region and their preliminary interpretation., TAO, Vol. 9, No. 3, 509-532.

ODB CD003: gravity/hsu grav 1am.ard



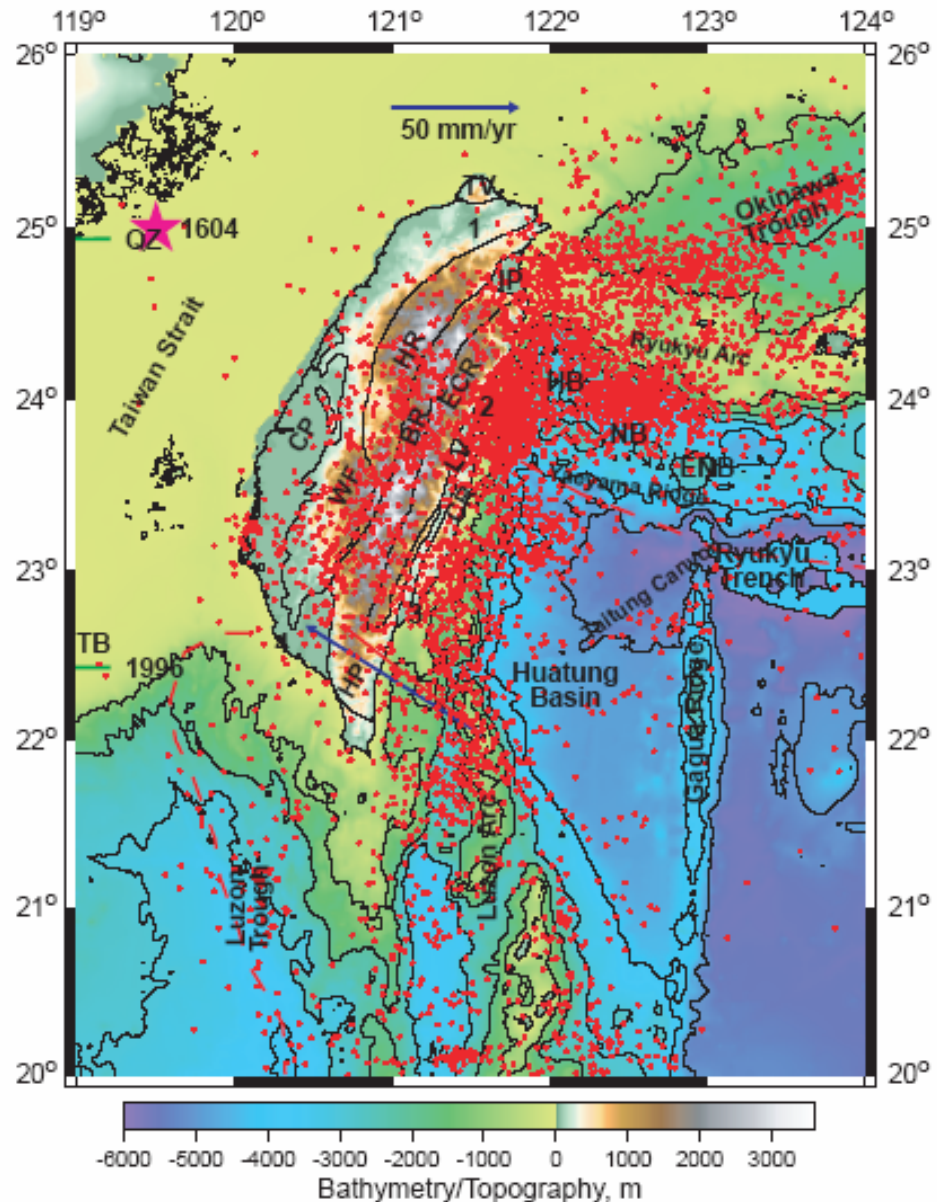
(A) Shear-wave splitting (Rau et al., 2000) showing trend parallel fast directions. Since source of splitting must be in the mantle, does this parallelism imply vertical coherence of deformation through the upper 300-400 km? (B) Bouguer gravity. Note that the high Central Range is not associated with a gravity minimum. Also Hengchun Peninsula is an area of positive Bouguer anomaly.

TAIWAN SEISMICITY (1991.1 - 2001.10)

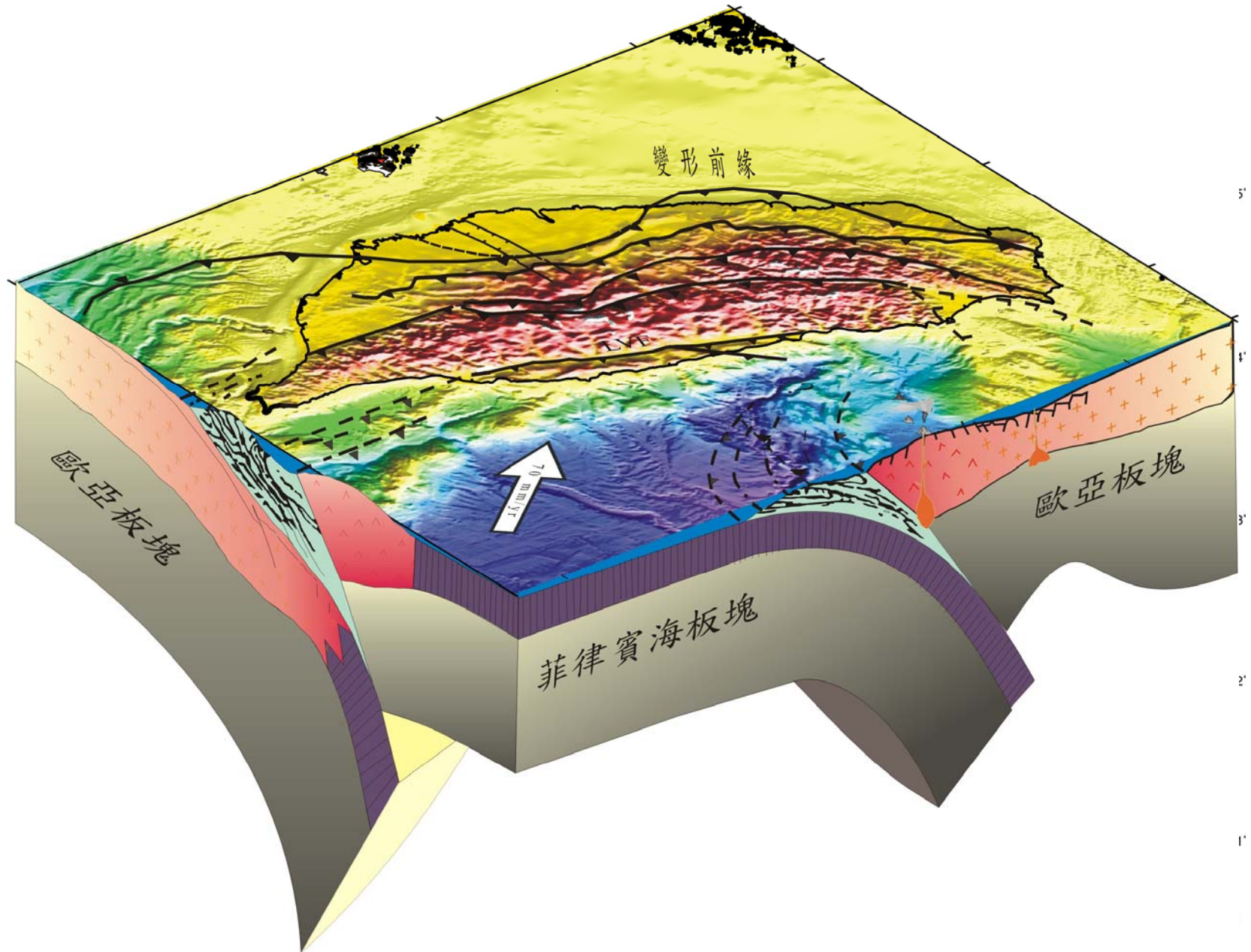


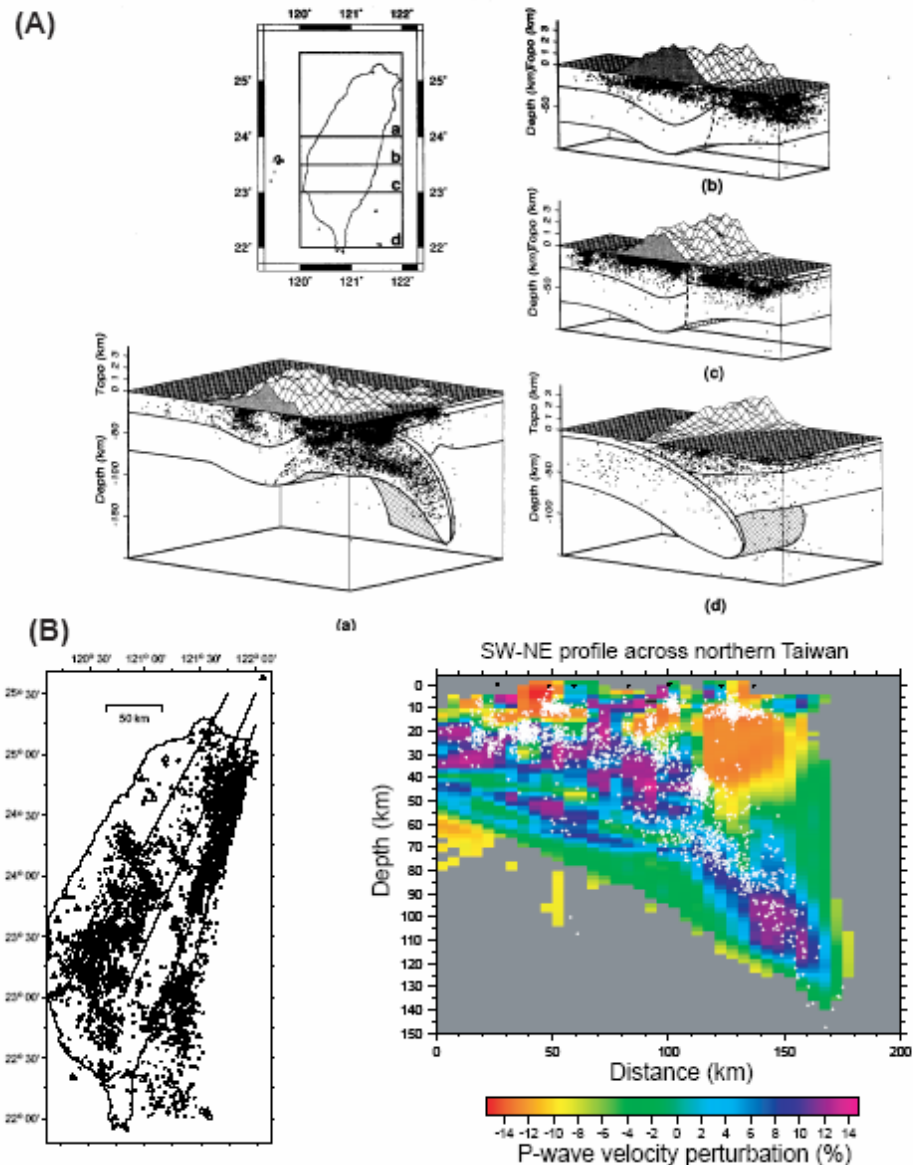
台灣地區 1991-2001 年地震震央 分布圖

Tectonic map of Taiwan showing the Ryuku and Manila Trenches and their associated arcs. The star in the upper left is the estimated epicenter of the 1604 M=8 earthquake and 1996 refers to the M=6.5 earthquake in 1996.



台灣的地震分布和地體構造

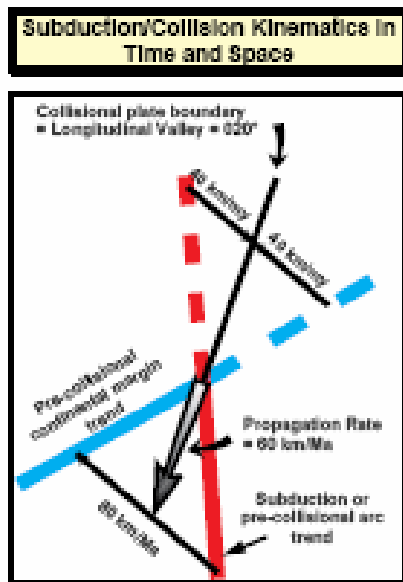




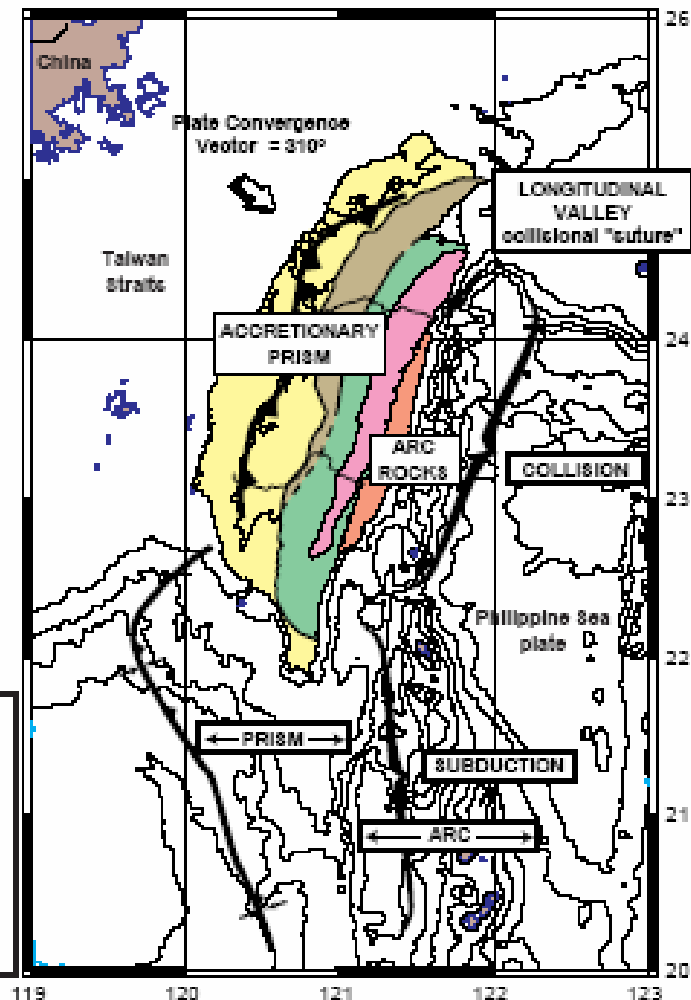
Block geometry of plates in Taiwan region. (A) Synthesis of seismicological and geophysical data showing major subsurface structures. Structures are superposed on 3D seismic foci. Depth of crustal features from seismic tomography. The WNW motion of the Philippine Sea plate led to both northward subduction of PSP and the collision of PSP and Eurasian plate lithospheres, resulting in thickening of the crust and lithospheres (Wu et al., 1997). (B) Results from Benz's finite difference ray tracing tomography software. Section along east side of Taiwan shows well-defined high velocity zone where the earthquakes are. Result by Wu and Benz (unpublished) used >5000 earthquakes (in map) recorded by Central Weather Bureau of Taiwan. Bending of subducting plate begins south of 24°N, i.e., south of the northern end of the Longitudinal Valley.

Figure 5

(A)

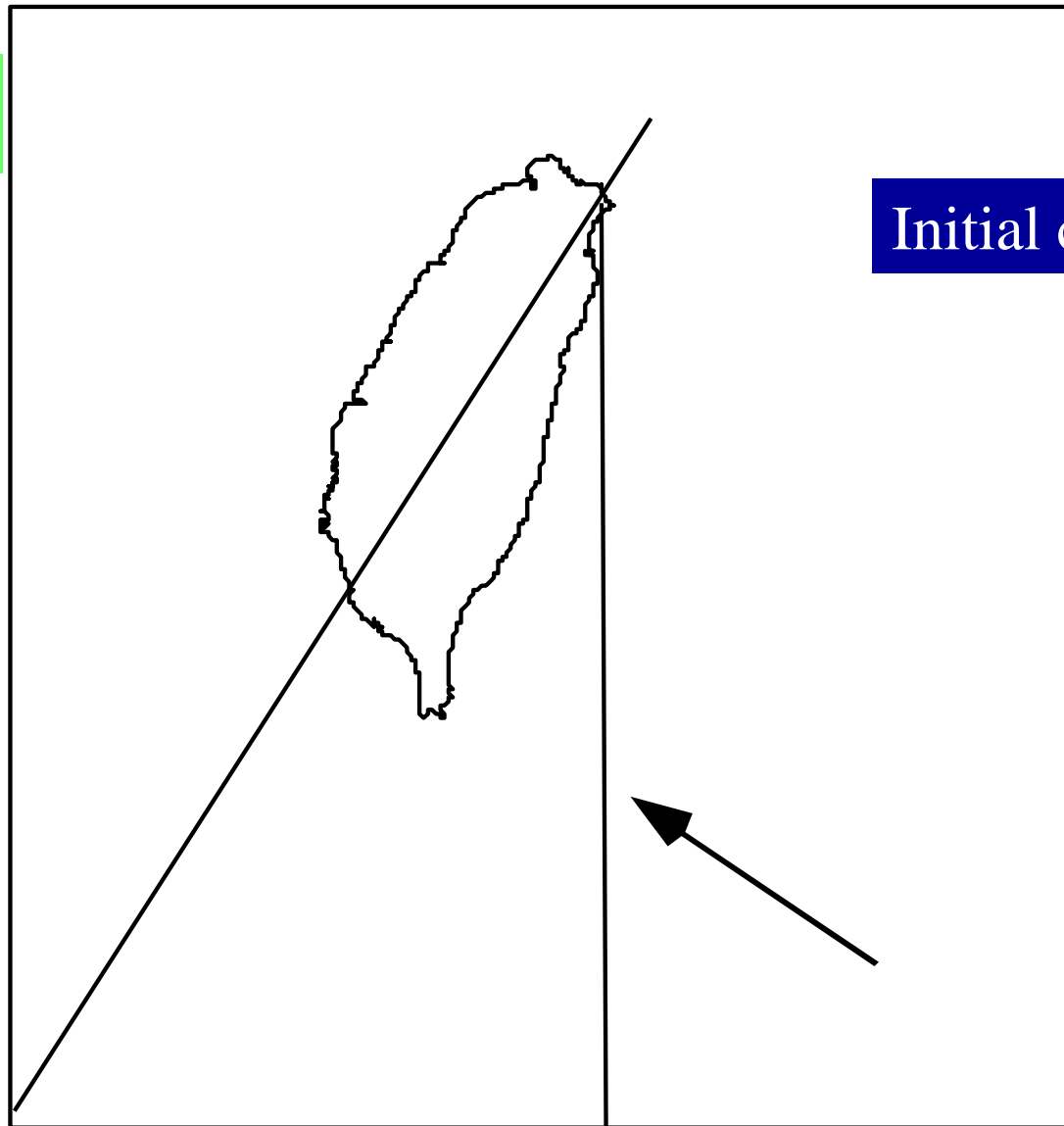


(B)



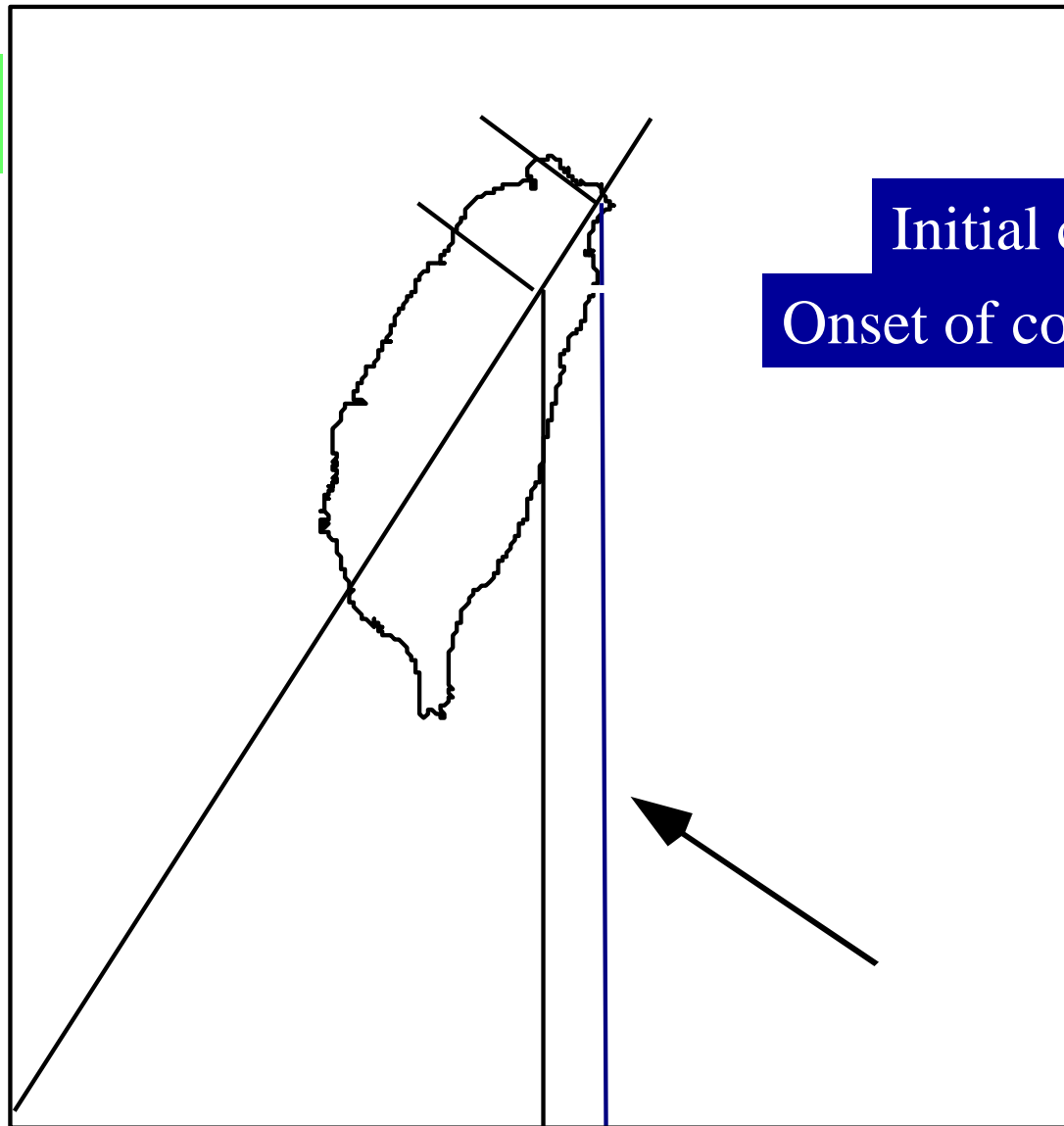
Background information for the Taiwan arc-continent collision. (A) Plate kinematic model. (B) Tectonics and geology of the Taiwan arc-continent collision. The kinematic model indicates a propagation rate of 60 km/my and nearly equal shortening rates (~40 km/my) in the accreting arc and continental margin.

6 Ma



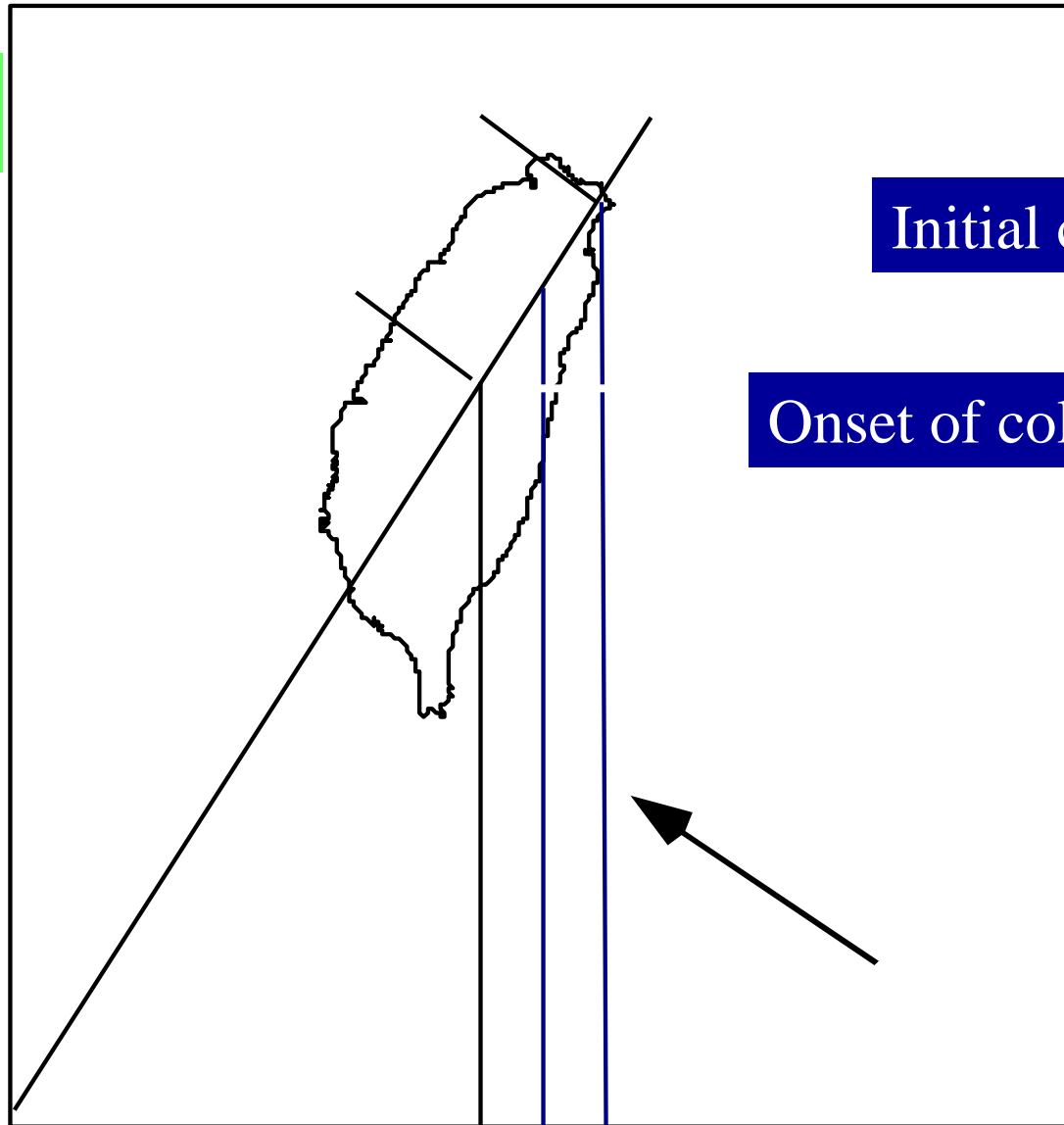
Initial collision

4 Ma



Initial collision
Onset of collision

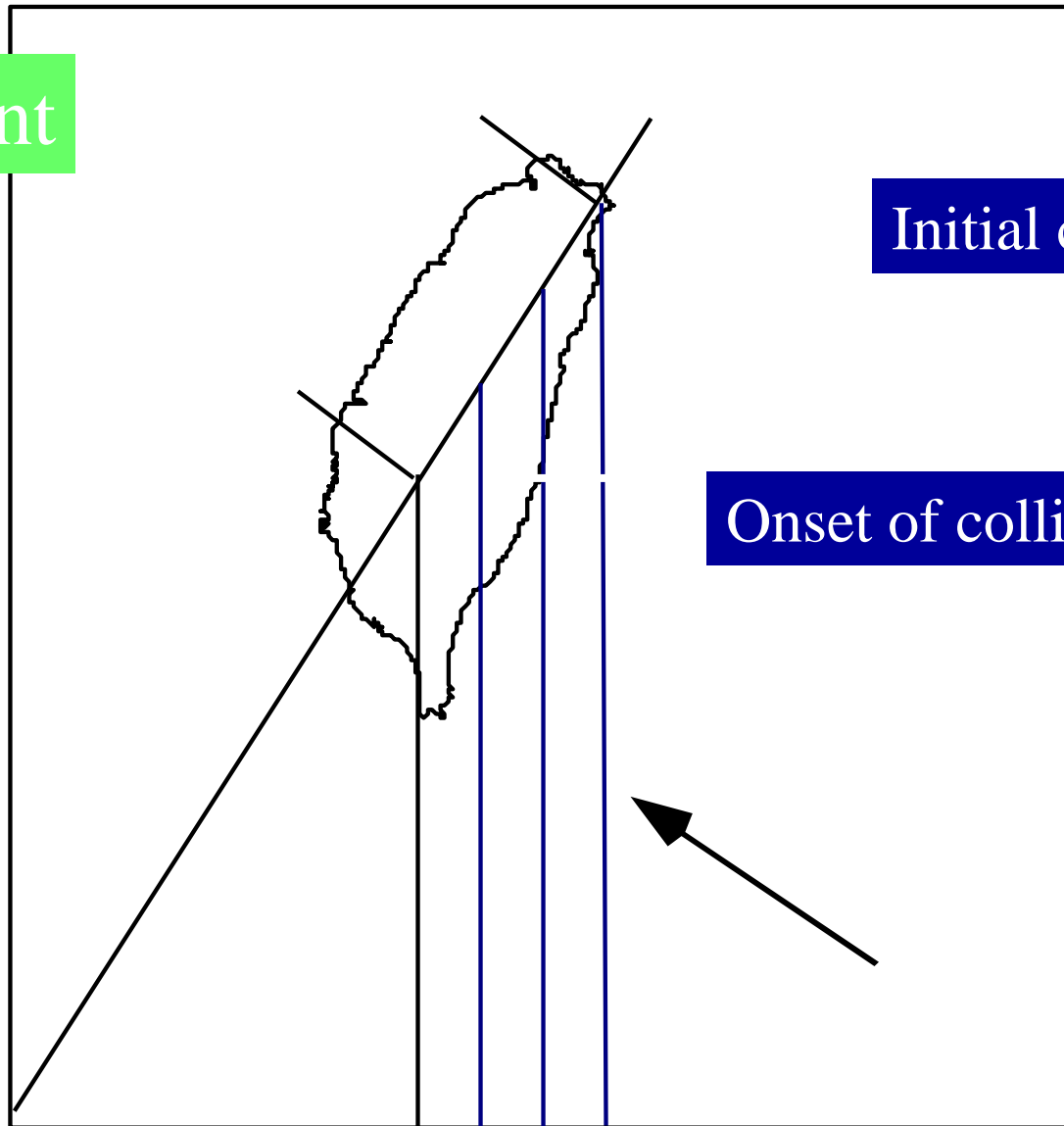
2 Ma



Initial collision

Onset of collision

Present



Initial collision

Onset of collision

Current Conceptual Models

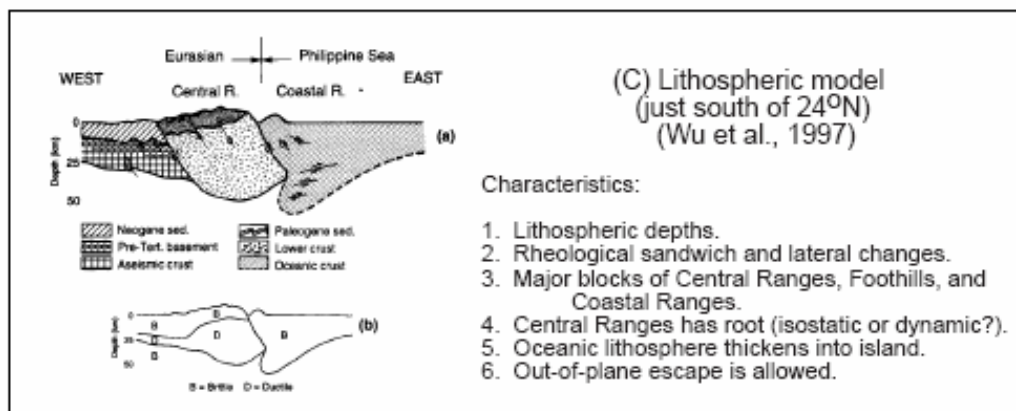
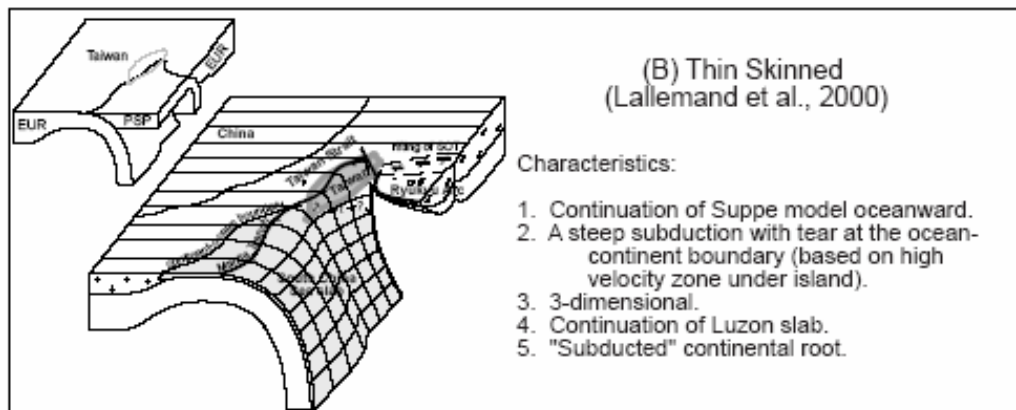
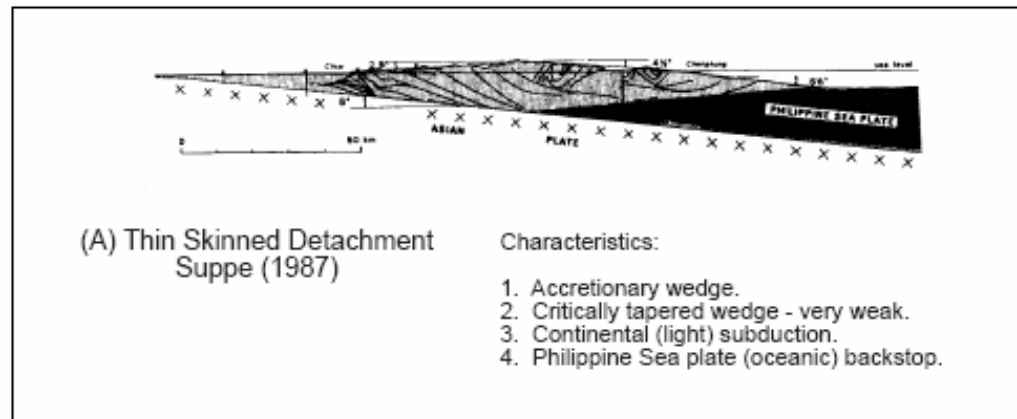
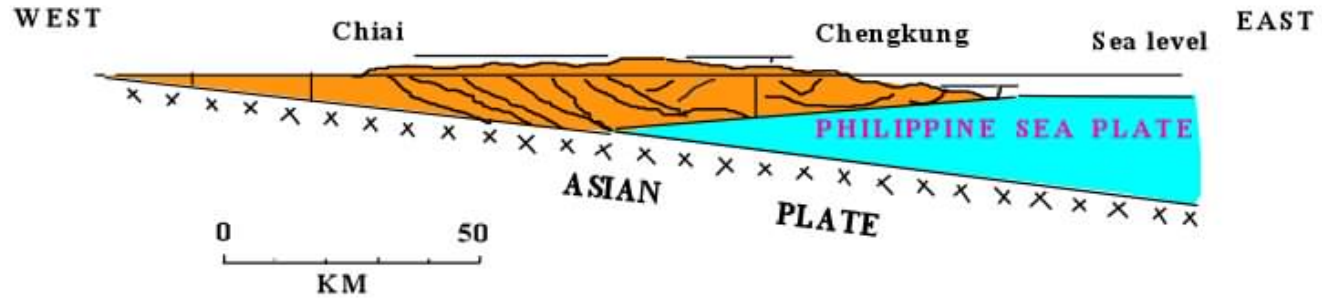
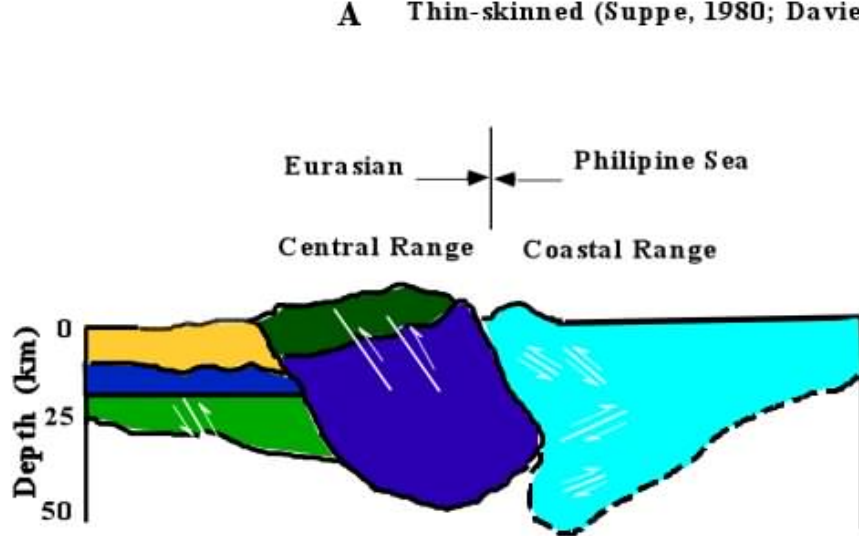


Figure 15

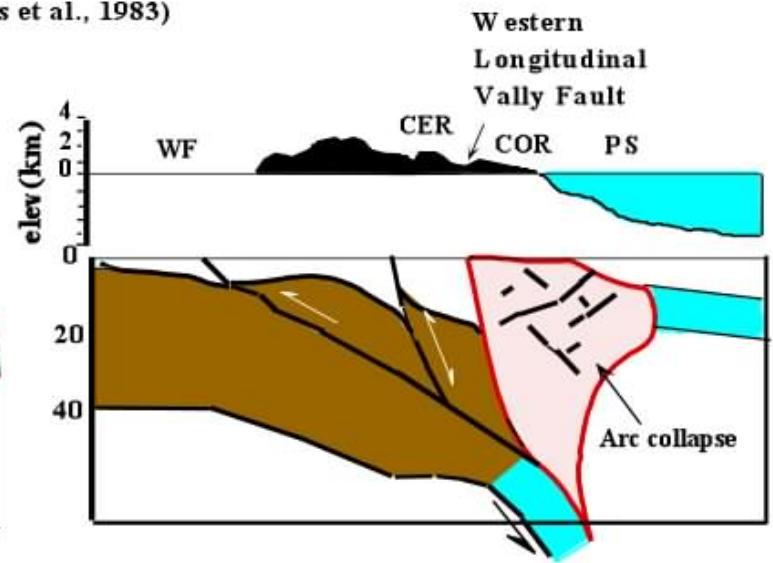
Geodynamic Models of Taiwan Mountain Belt



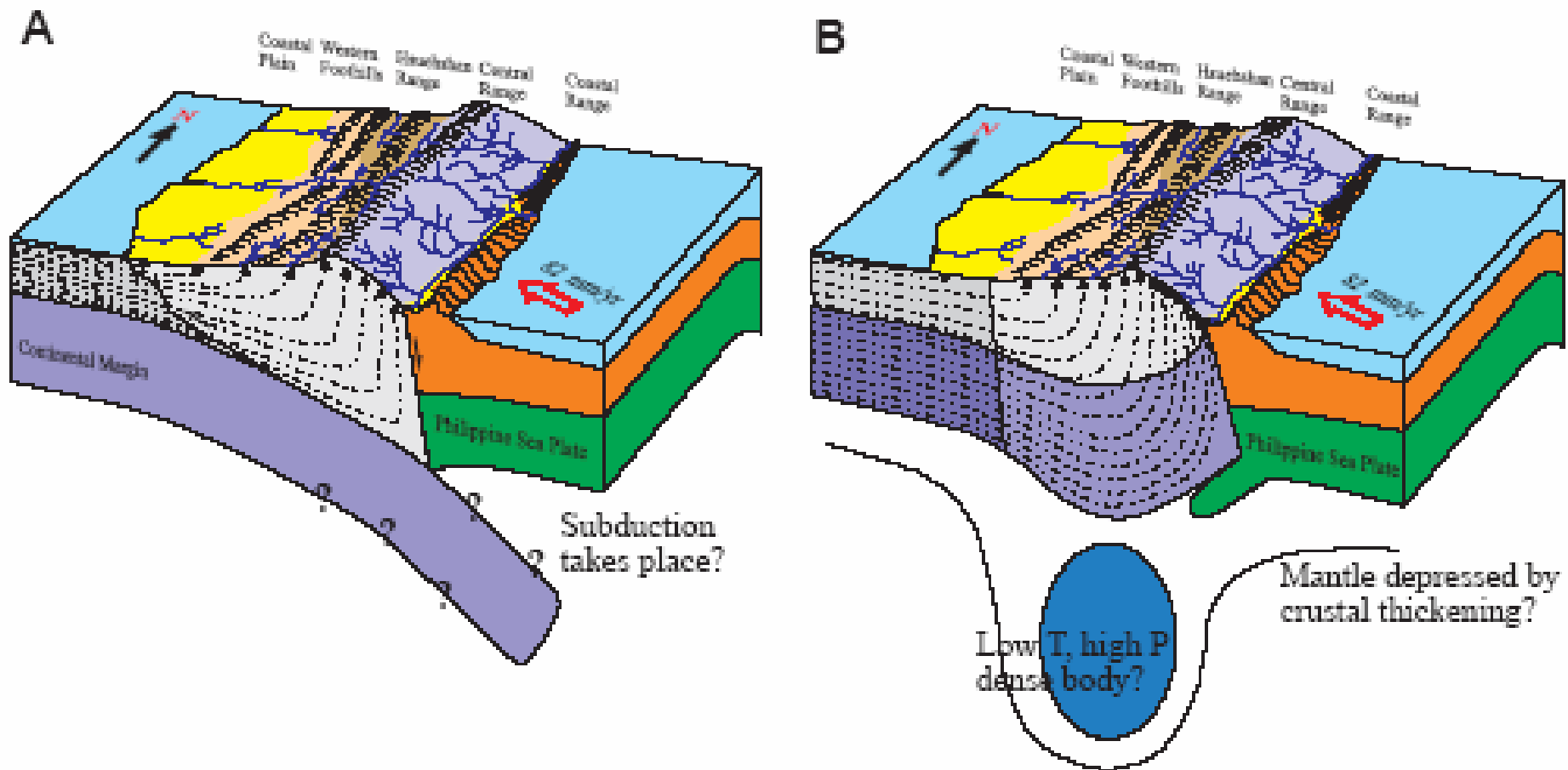
A Thin-skinned (Suppe, 1980; Davies et al., 1983)



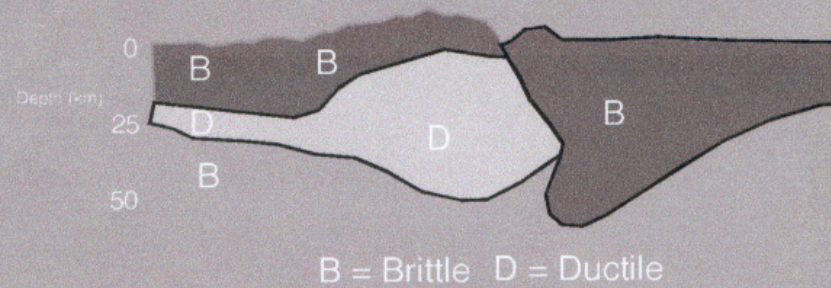
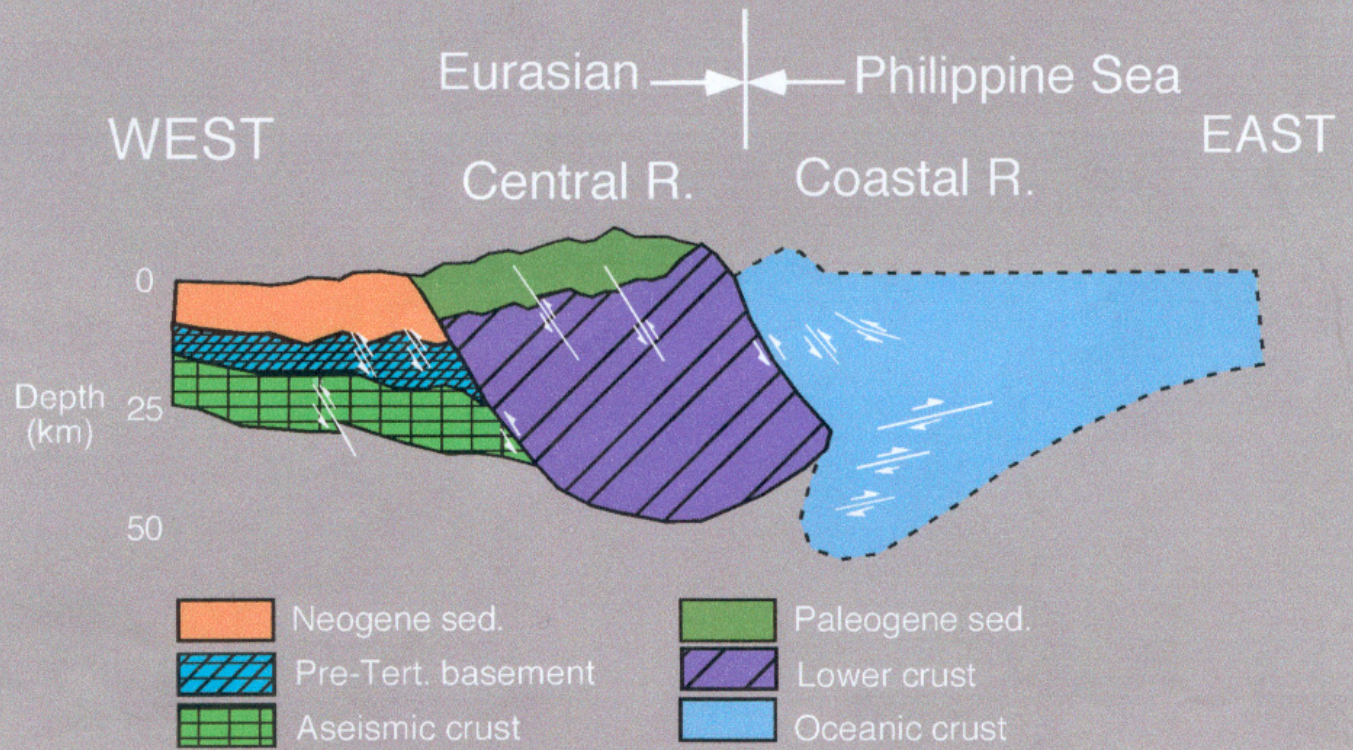
B Lithospheric thickening (Wu, et al., 1997)



C Crustal extension in the Backbone Range (Byrne, 1995)

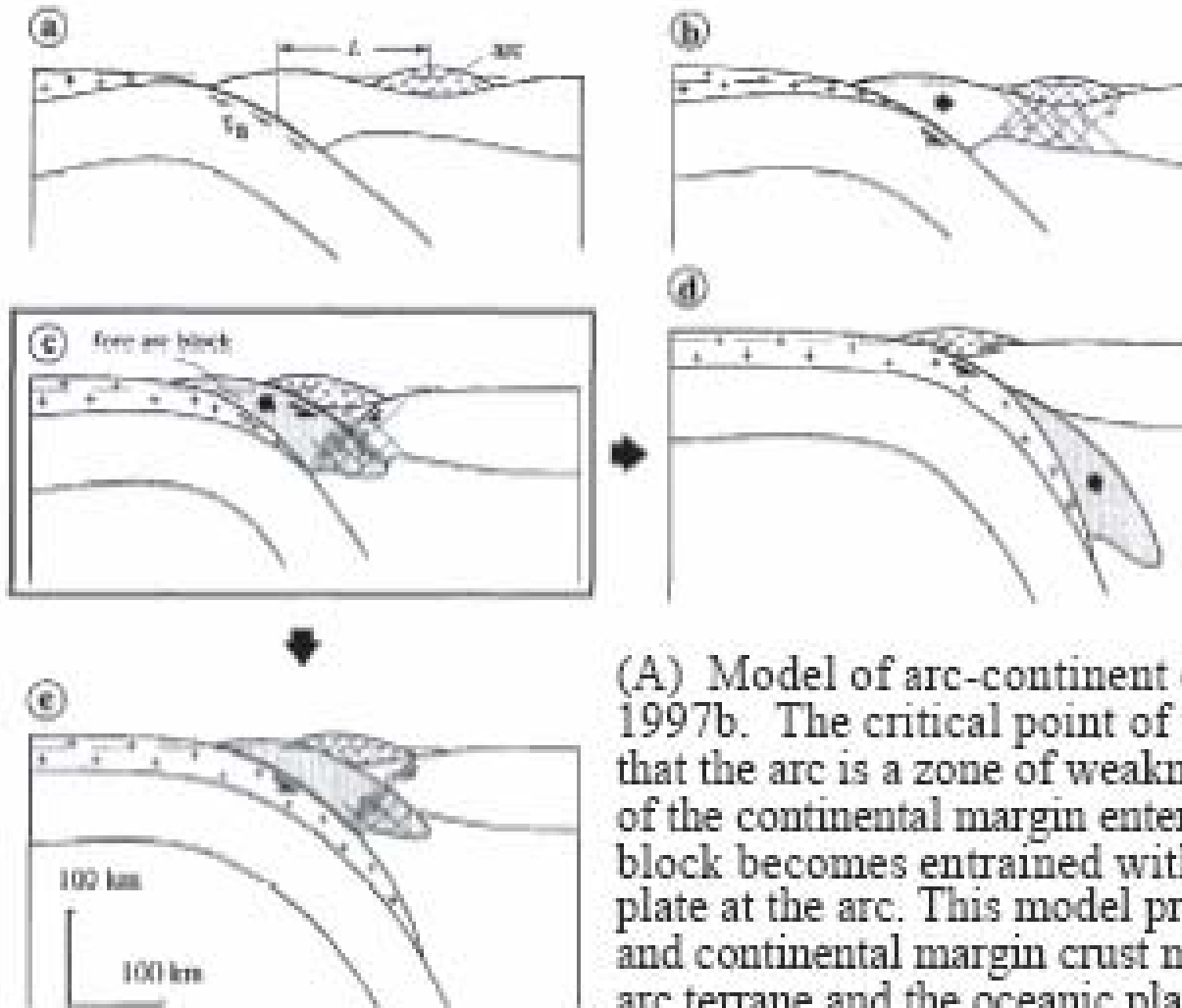


End-member models for arc-continent collision as applied to the Taiwan orogen. (A) Thin-skinned with subduction. (B) Pure shear with no subduction. Different kinematics exist within the mountain belt and for both models information regarding mantle structures is lacking.



After Wu et al. (1997)

Other Geodynamic models of Taiwan



(A) Chemenda model

(A) Model of arc-continent collision from Chemenda et al., 1997b. The critical point of this lithospheric-scale model is that the arc is a zone of weakness, so that when thickened crust of the continental margin enters the subduction zone the forearc block becomes entrained with it and detaches from the upper plate at the arc. This model predicts that both the forearc block and continental margin crust may be found beneath the remnant arc terrane and the oceanic plate

(B) Malavieille model

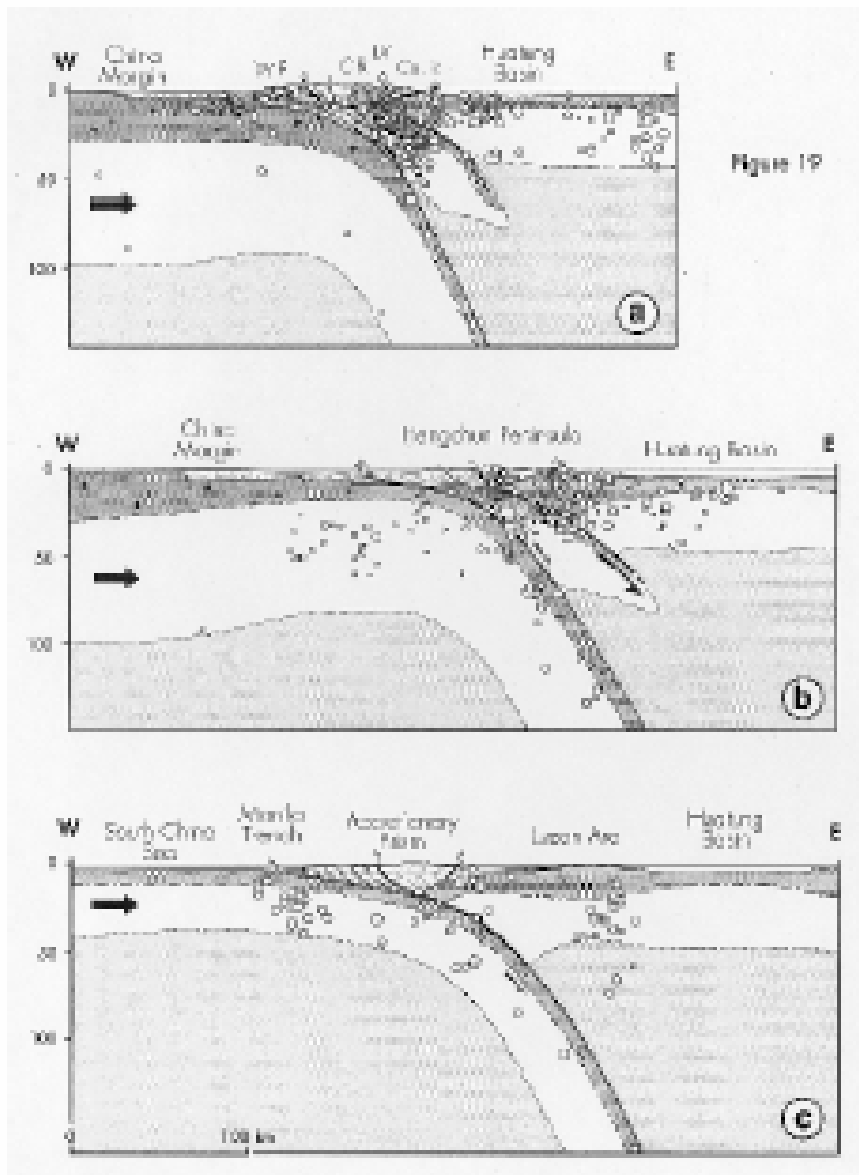


Figure 19

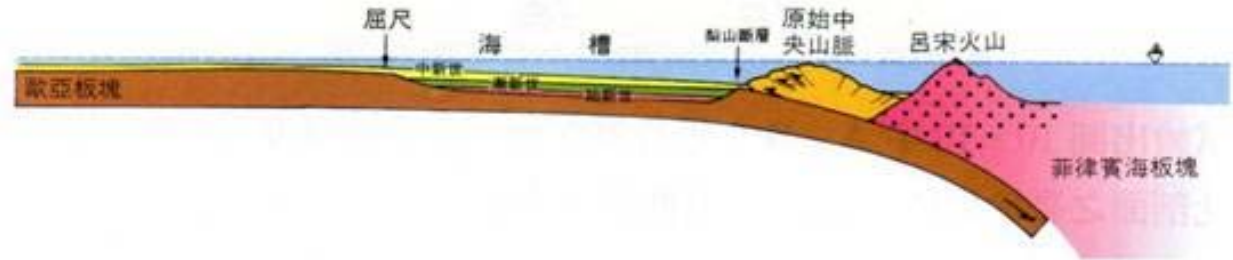
(B) Model of Taiwan development from Malavieille et al. (2002). This model adopts the concepts of the Chemenda model (above) and includes features specific to Taiwan. Part c (bottom) depicts the possible tectonic configuration south of Taiwan, near our proposed Transect 6, featuring a doubly vergent accretionary prism centered above the junction of the forearc basement and the subducting Eurasia oceanic basement.

Part b, across the Hengchun Peninsula, shows the forearc block detached from the arc and entrained with the subducting continental margin lithosphere.

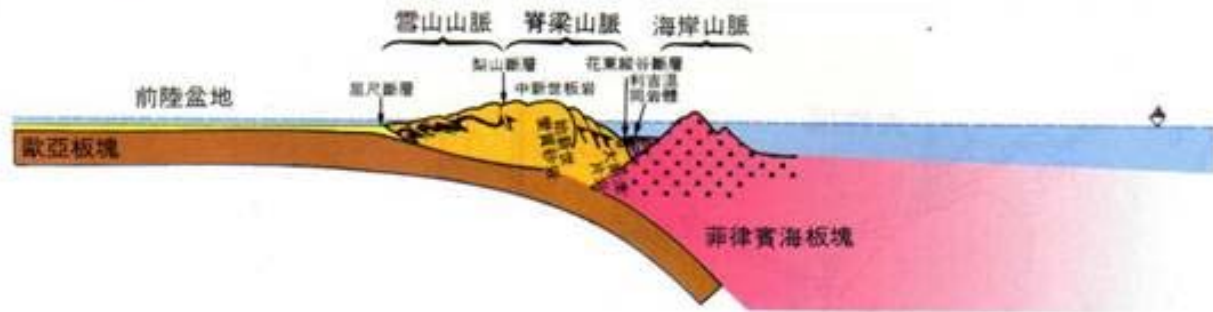
Part a shows the possible configuration of the mature collision. At this stage underthrust continental crust is being underplated beneath the Central Range. Note that all stages of the model predict the presence of a Eurasia plate slab, including significant underthrusting of the continental margin crust and lithosphere.

台灣式碰撞

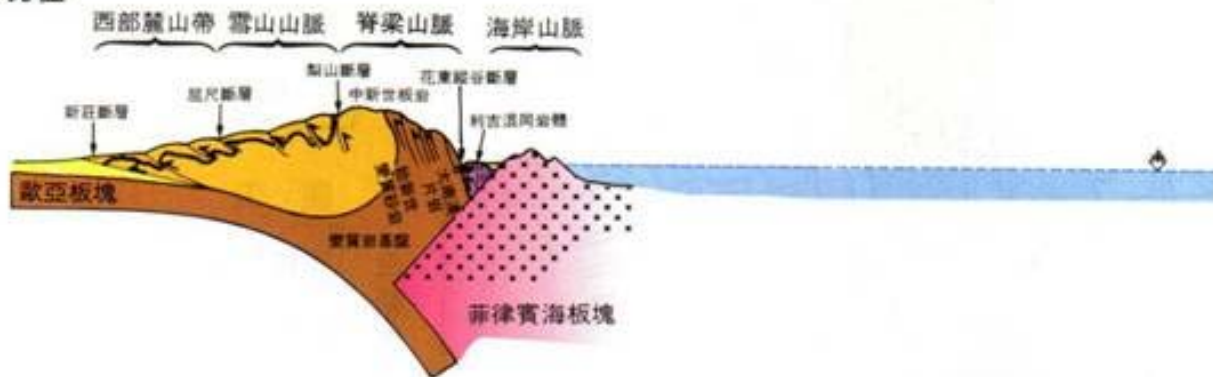
(a) 中新世晚期 (650 萬年前)



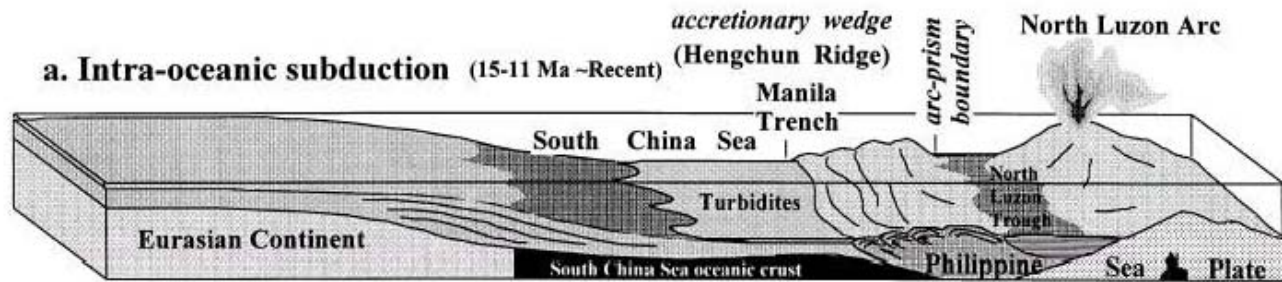
(b) 上新世晚期 (250 萬年前)



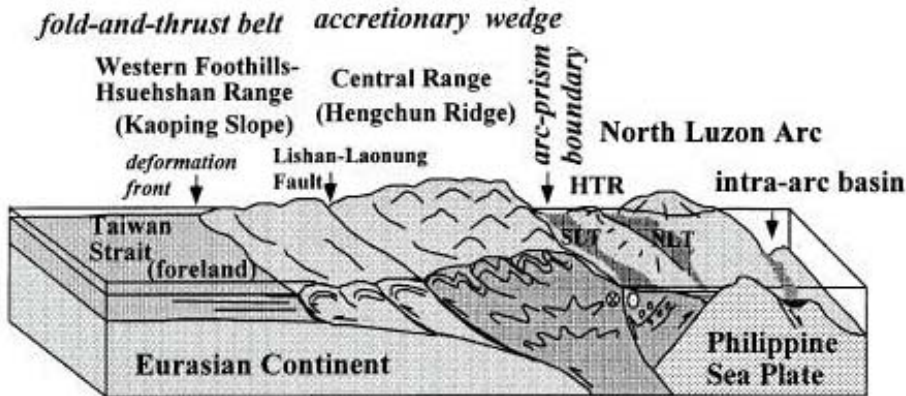
(c) 現在



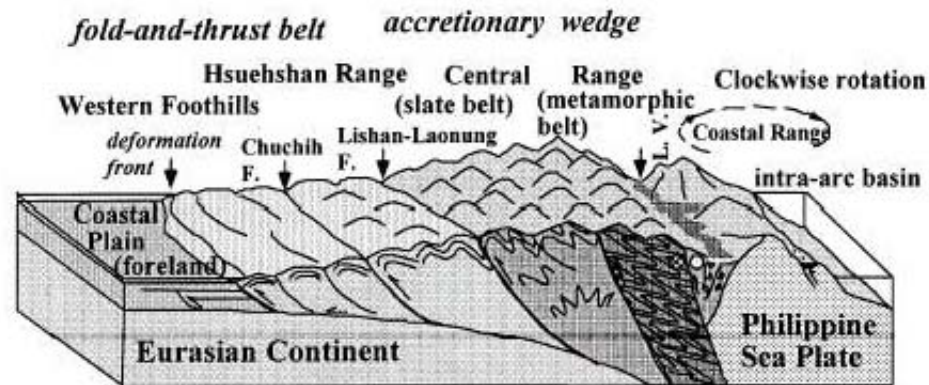
造山帶構造演化的四個過程



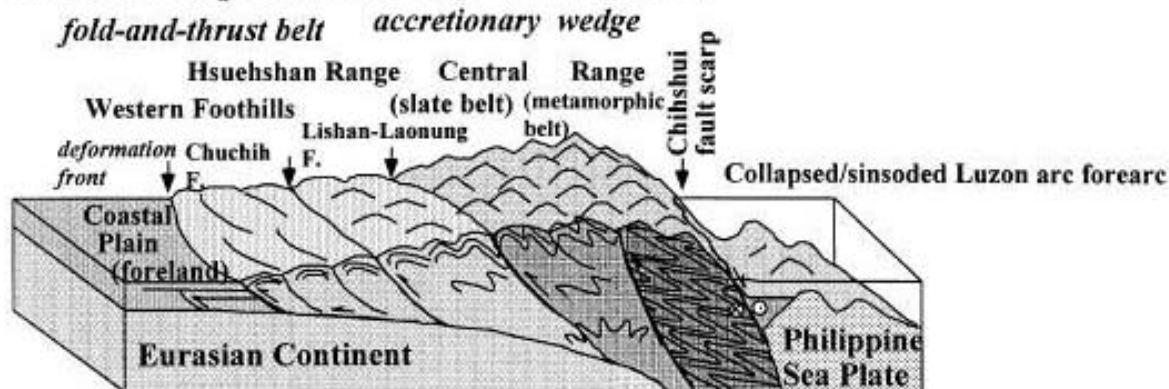
b. Initial arc-continent collision (5 Ma ~Recent)

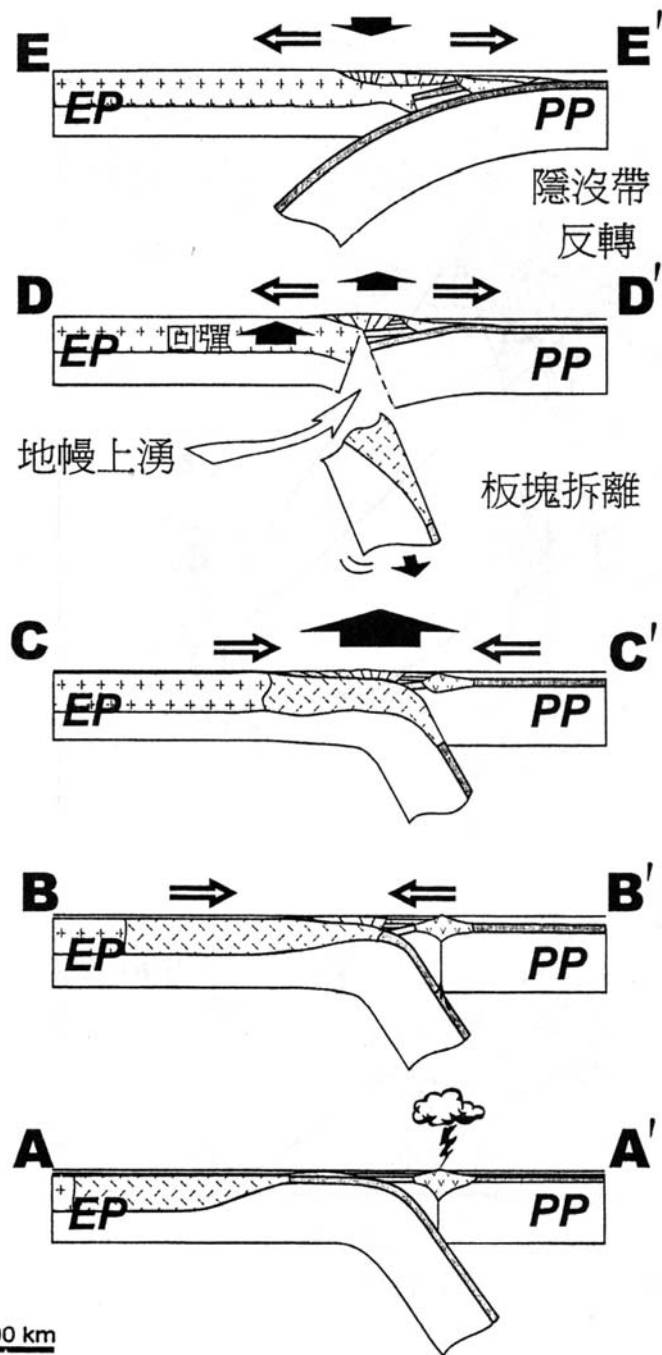
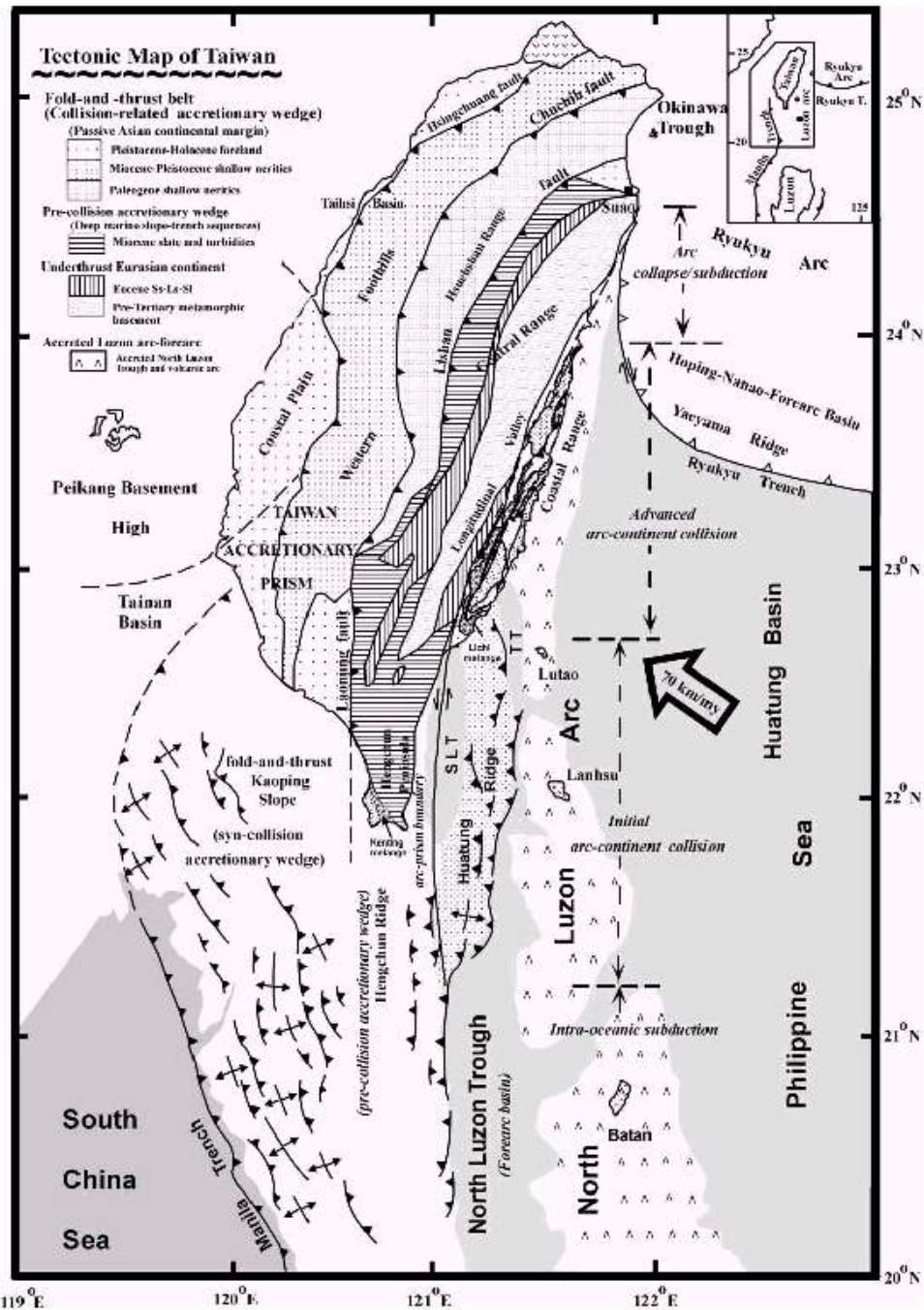


c. Advanced arc-continent collision (2 Ma ~Recent)



d. Arc collapse/subduction (1-2 Ma ~Recent)





Evidences of think-skinned Tectonics

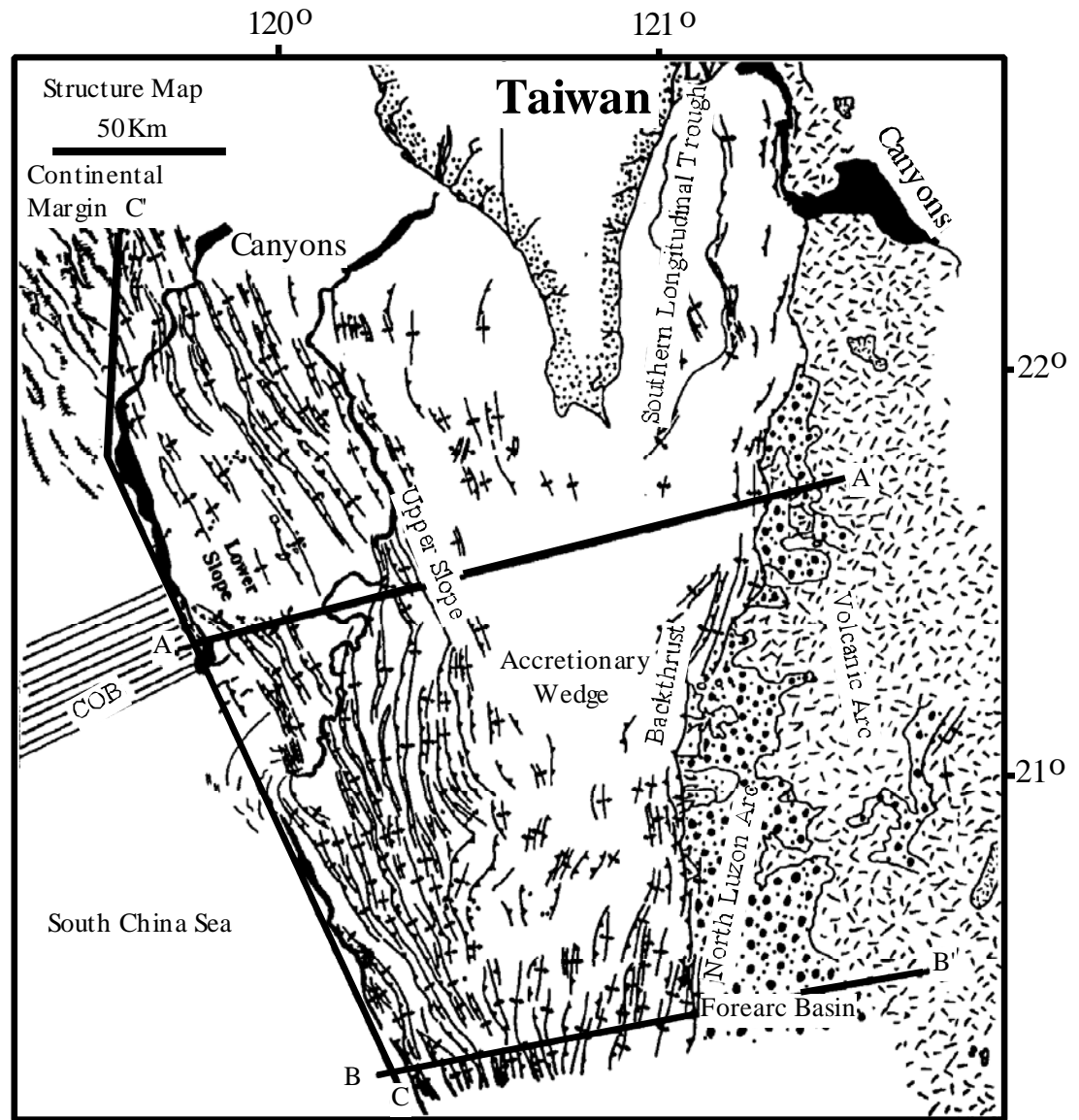
Pros:

- Southern Offshore Taiwan
- Onshore Field evidences
- P-wave velocity
- Earthquake data

Cons:

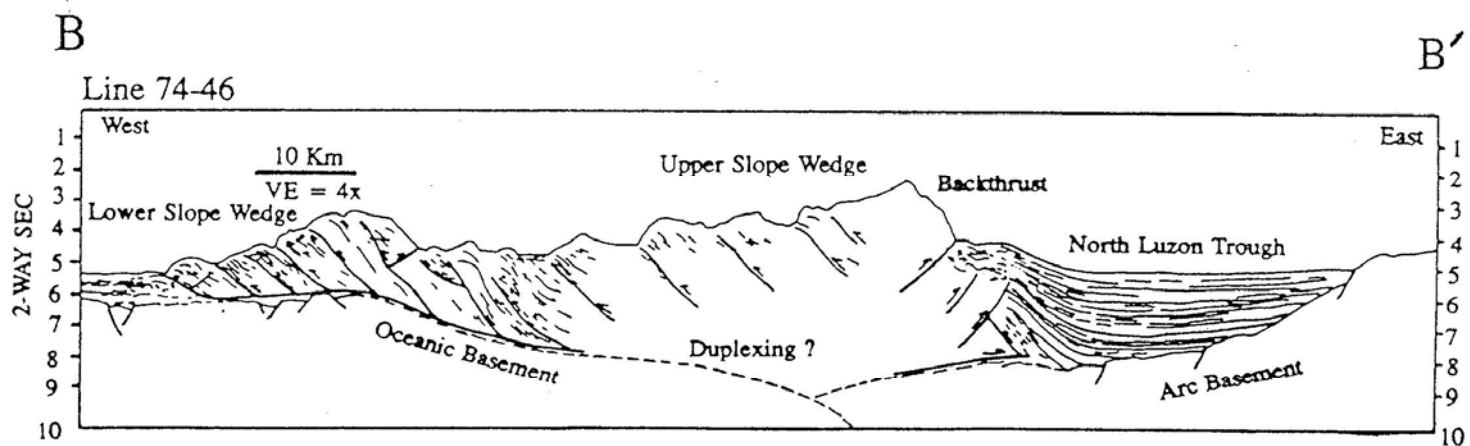
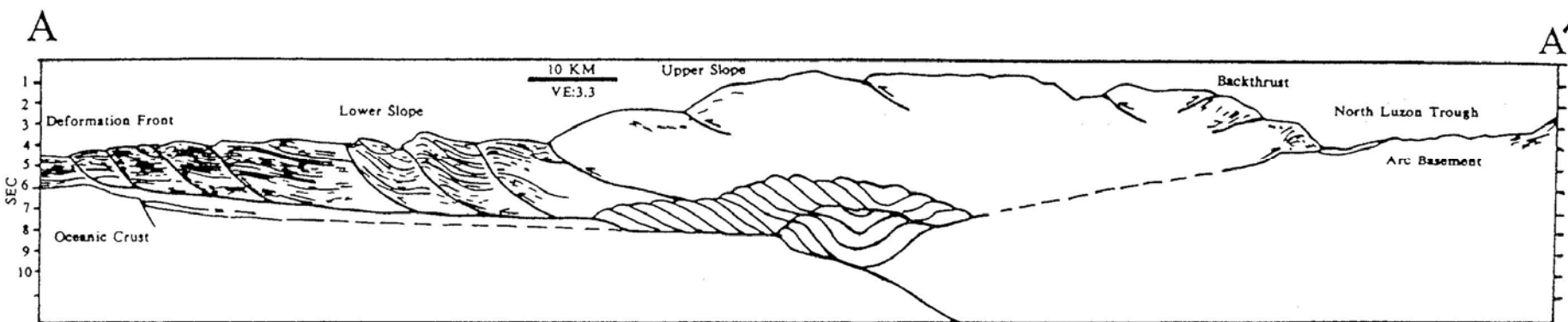
- Gravity modeling
- Earthquake data

**offshore
southwestern
Taiwan**



**Structure Map in the Region of the SeaMARC and 6-channel Seismic Survey
SW of Taiwan (Liu et al., 1992)**

Structures in southern offshore Taiwan



圖九、台灣西南海城代表性的震測剖面解釋顯示剛開始的弧陸碰撞(上圖)及隱沒作用(圖B)。由於構造複雜導致震測品質不佳,所以上部斜坡(upper slope)祇有少數斷層。脫序的逆衝斷層及重複堆疊的逆斷層係推測的構造(Reed et al.,1992)。

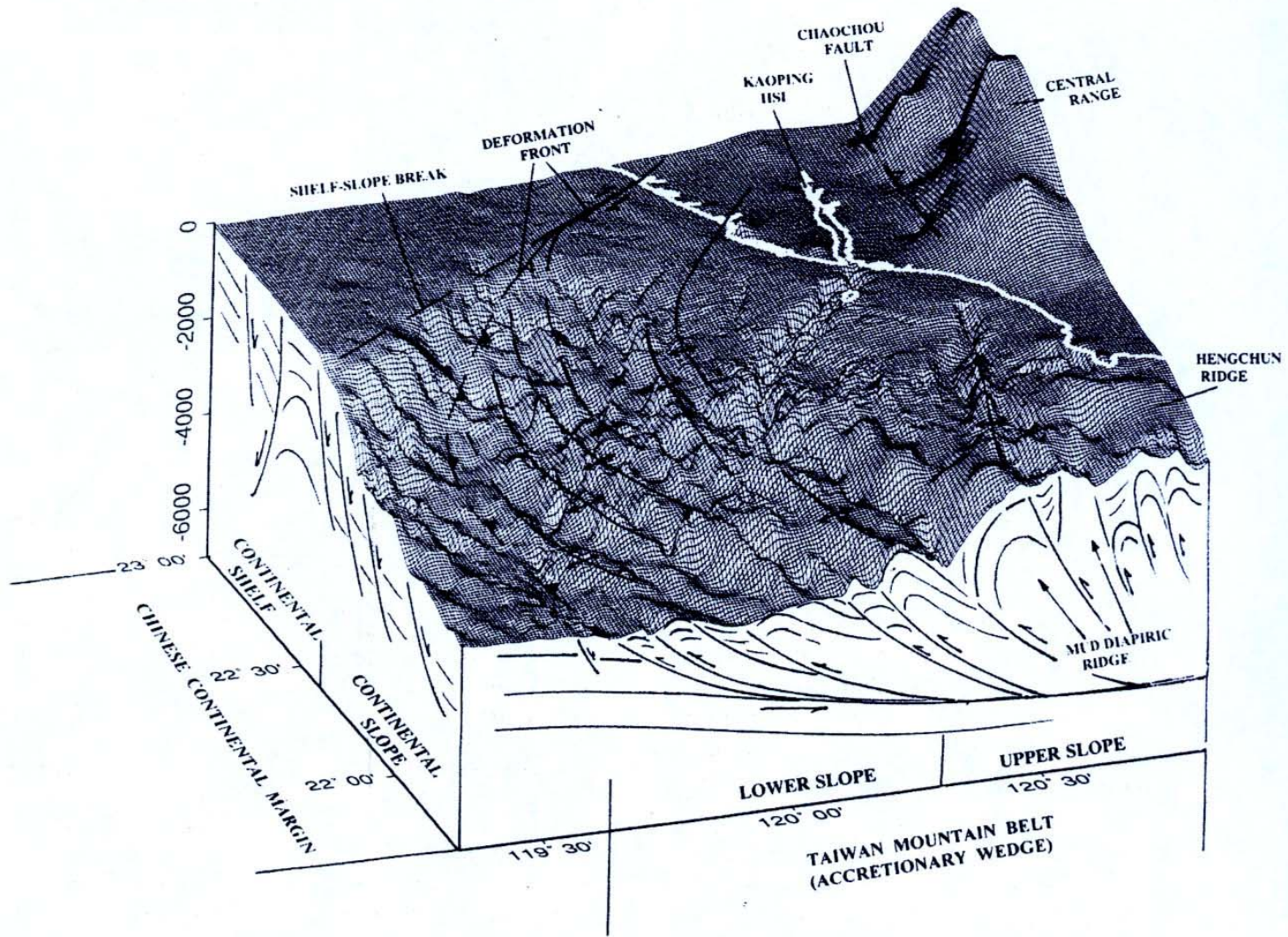
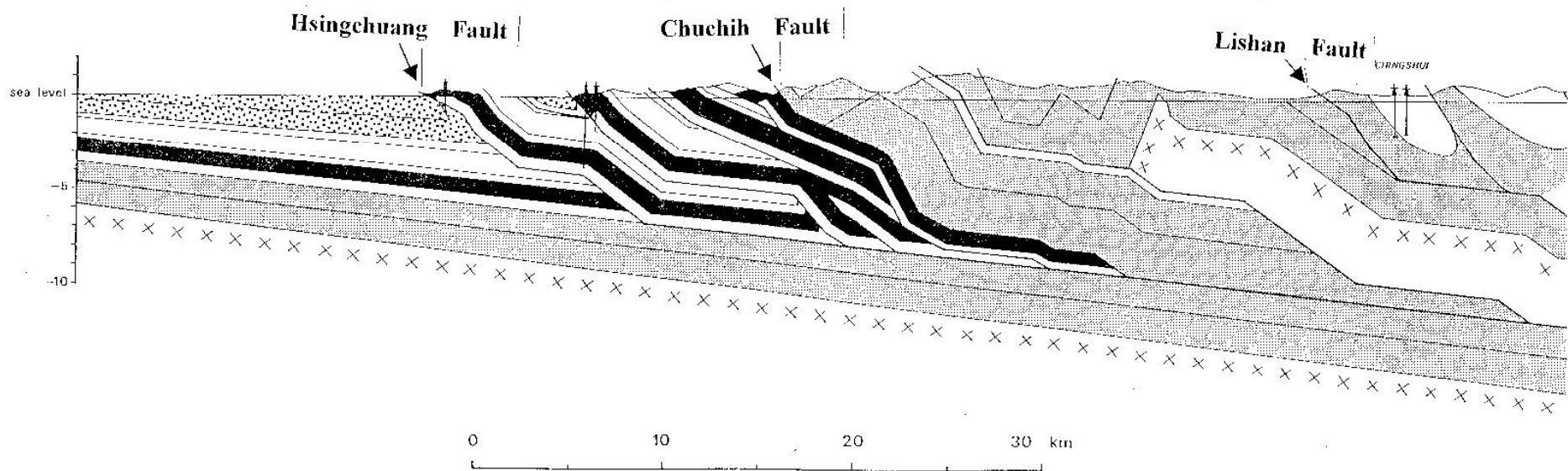
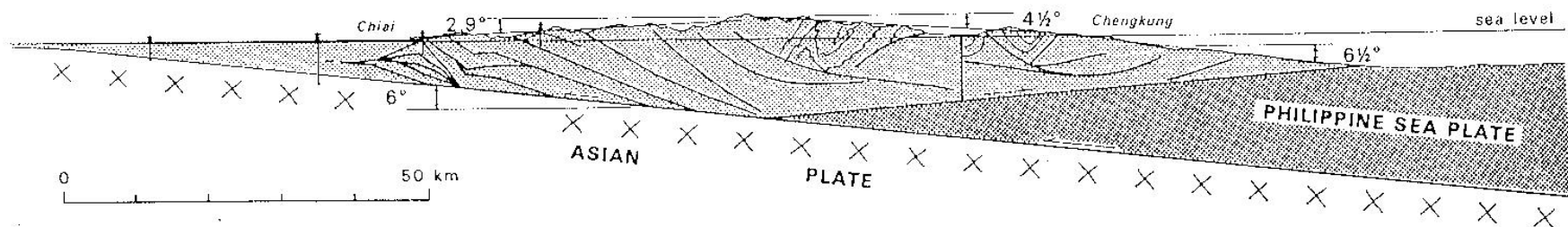


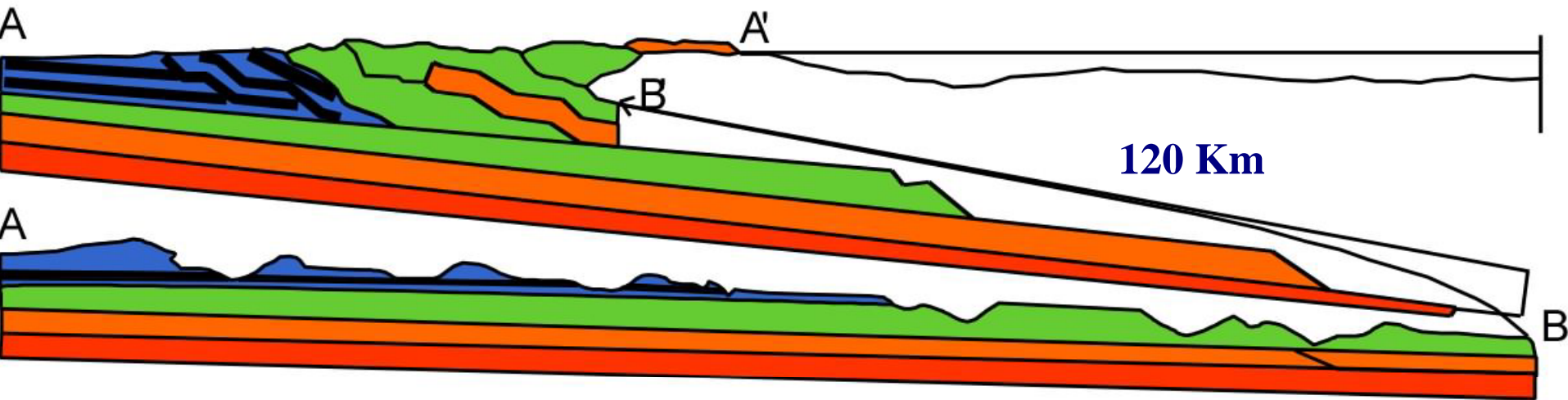
Fig. 8. A 3-dimensional structural interpretation of the Taiwan mountain belt for the area offshore southwestern Taiwan. Topographic relief of the anticlinal ridges in the lower slope domain indicates that the structural trend curves from NNW to NNE as these anticlinal ridges extended toward the Chinese continental margin. The overall structural pattern suggests that the deformation front aligns with the shelf-slope break as it approaches Tainan.

薄皮構造



圖十一、台灣山脈薄皮構造的岩體增積模式(Suppe, 1981)及台灣北部地質剖面圖(Suppe, 1980a)。麓山帶的範圍為介於新莊 (Hsinchuang) 及屈尺 (Chuchih) 斷層之間。

Retrodeformable cross-section [Suppe, 1980]



0 30km



Western Foothills: Sedimentary Sequences
(Late Oligocene to Early Pleistocene)

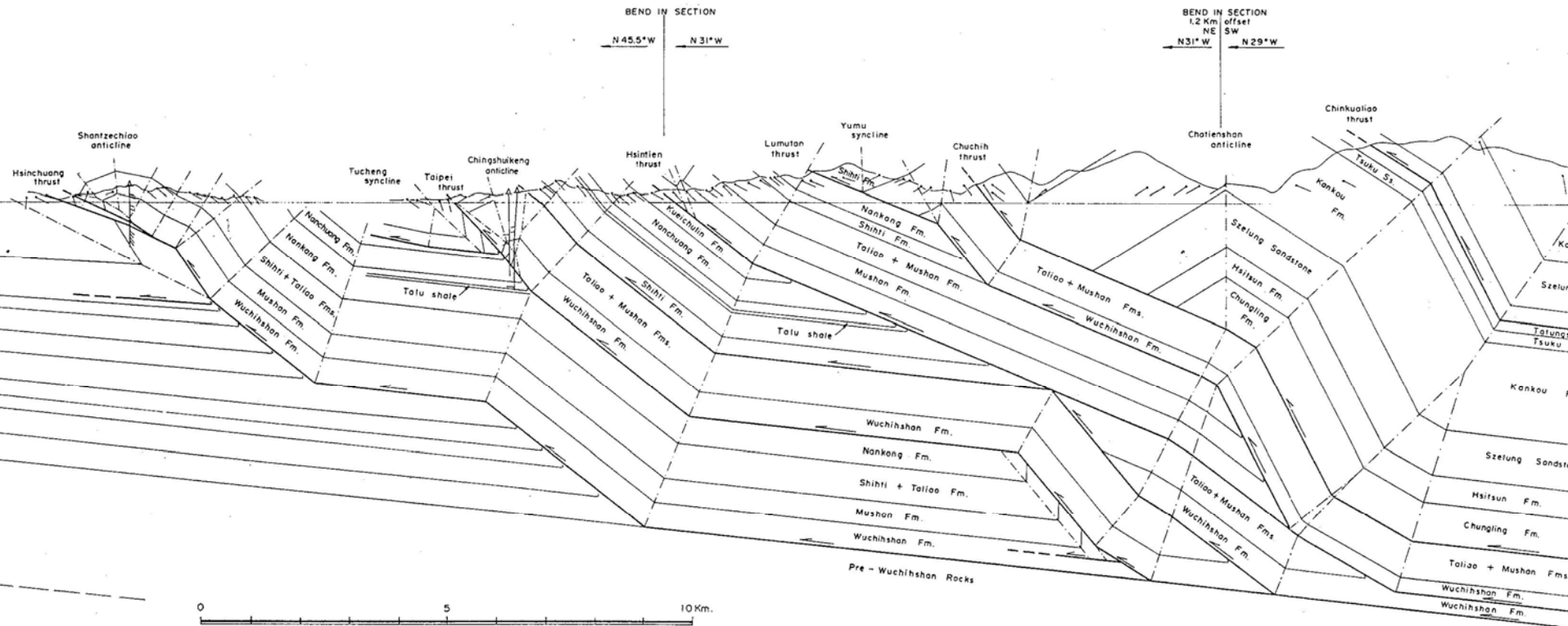


Western Central Range: Argillite-Slate Series
(Eocene to Middle Miocene)

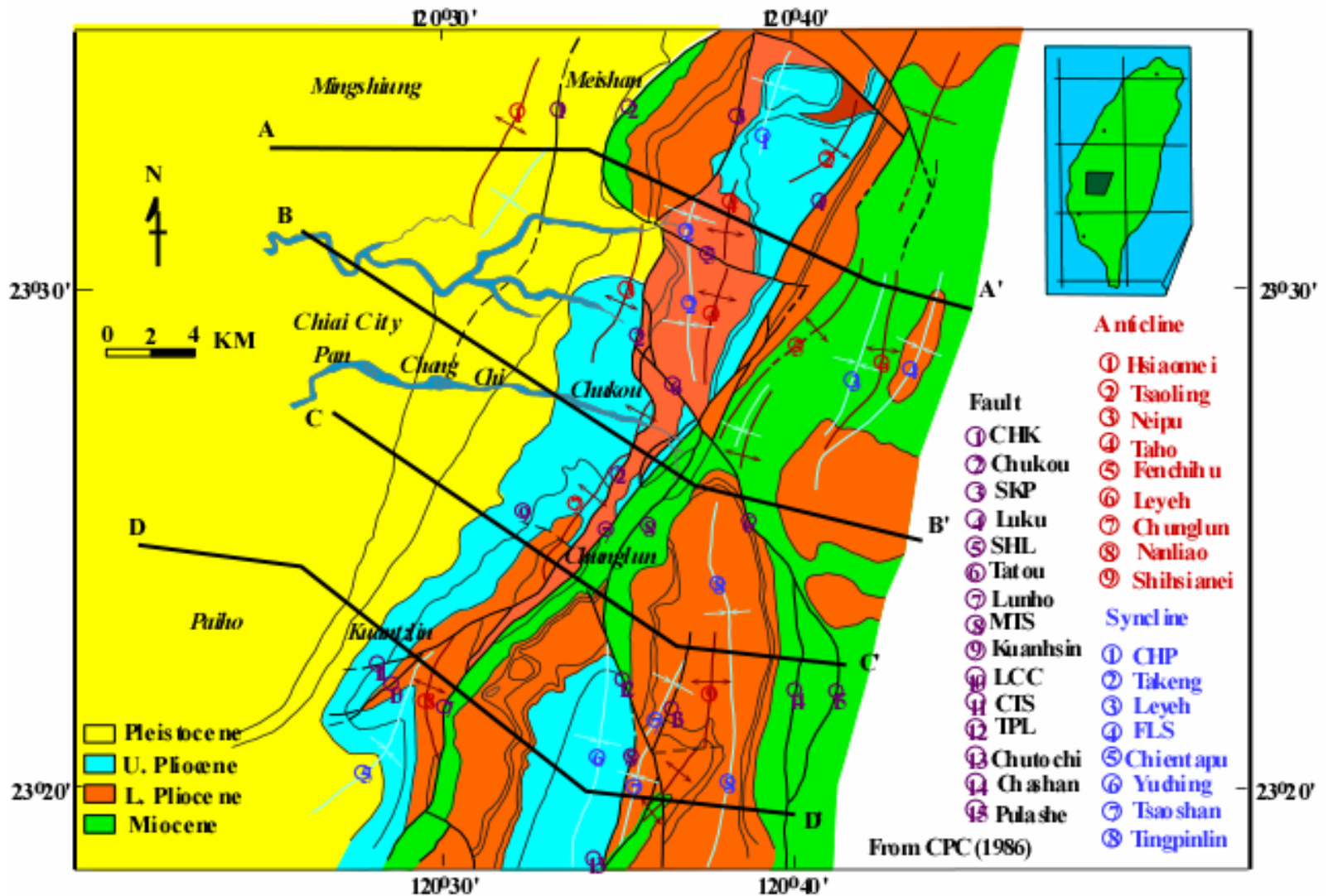


Eastern Central Range: Tananao Schists
(Permian-Triassic to Early Tertiary)

Structure Cross section across northern Taiwan as interpreted from Thin-skinned tectonics



Nanchuang Formation as a Decollement horizon in SW Taiwan

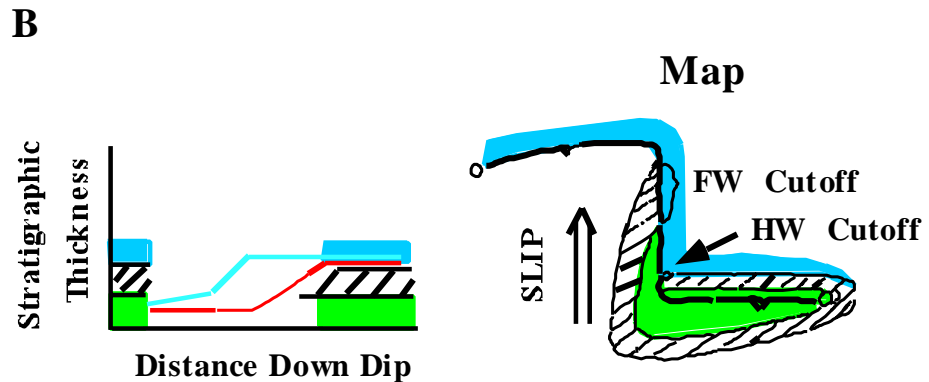
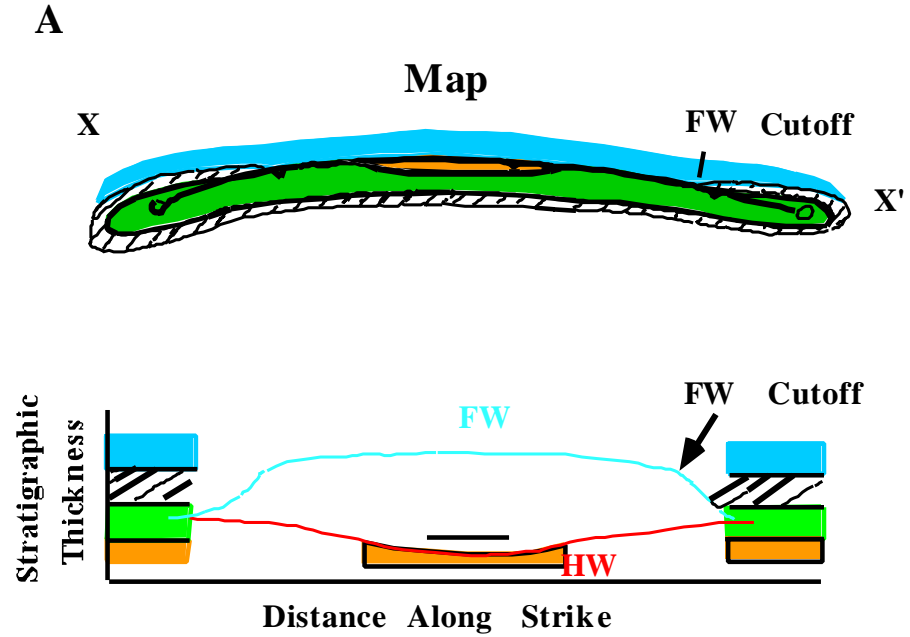


Decollement faults in western Taiwan Fold and Thrust Belt

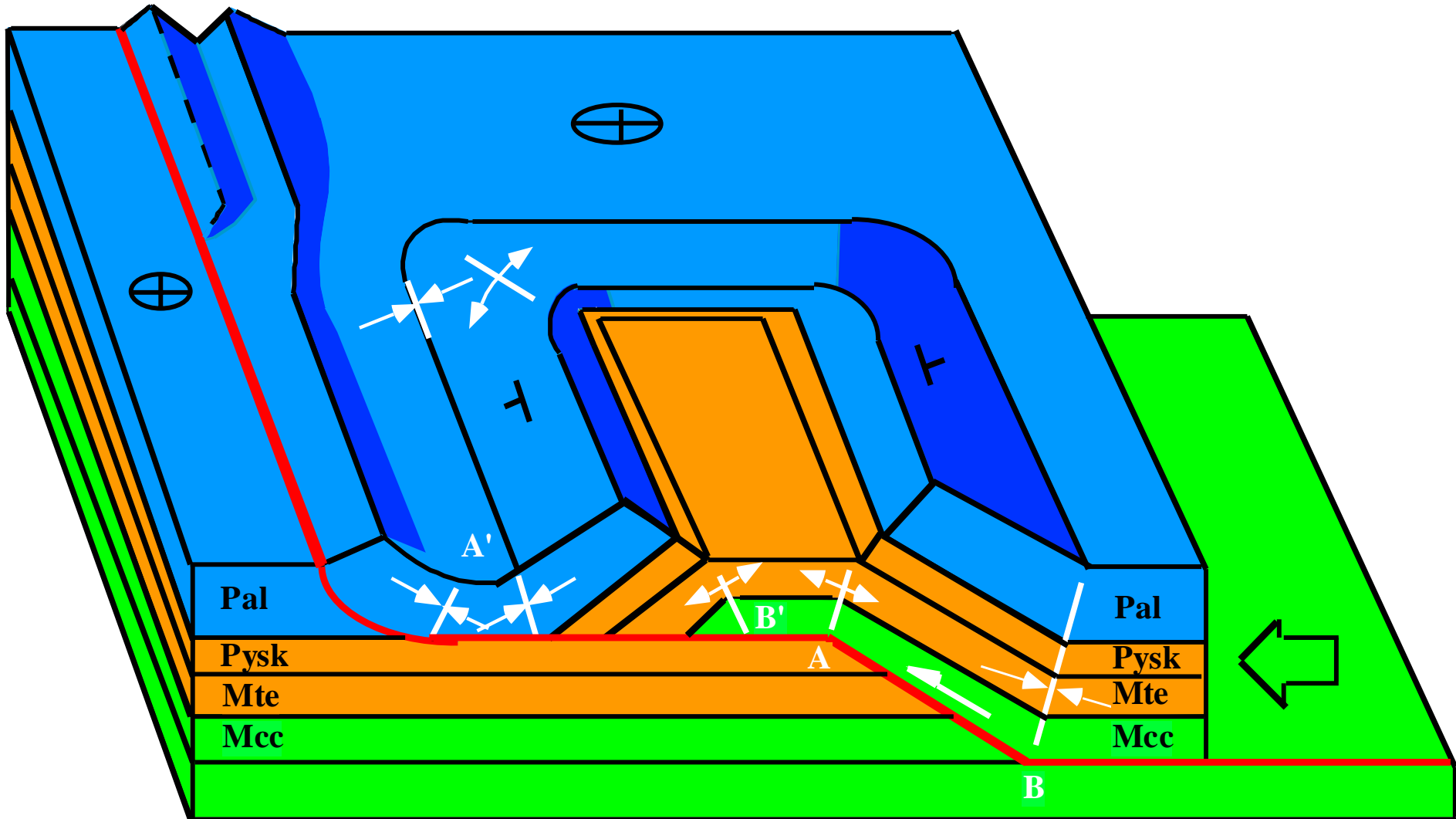
- Field Evidences
- Locations of detachments in Taiwan
 - Pre-Miocene : bottom of Wuchihshan Fm
 - Miocene: Nanchuang Fm.
 - Pliocene: Chinshui Fm.
- Depth of basal Detachment)~10 km depth

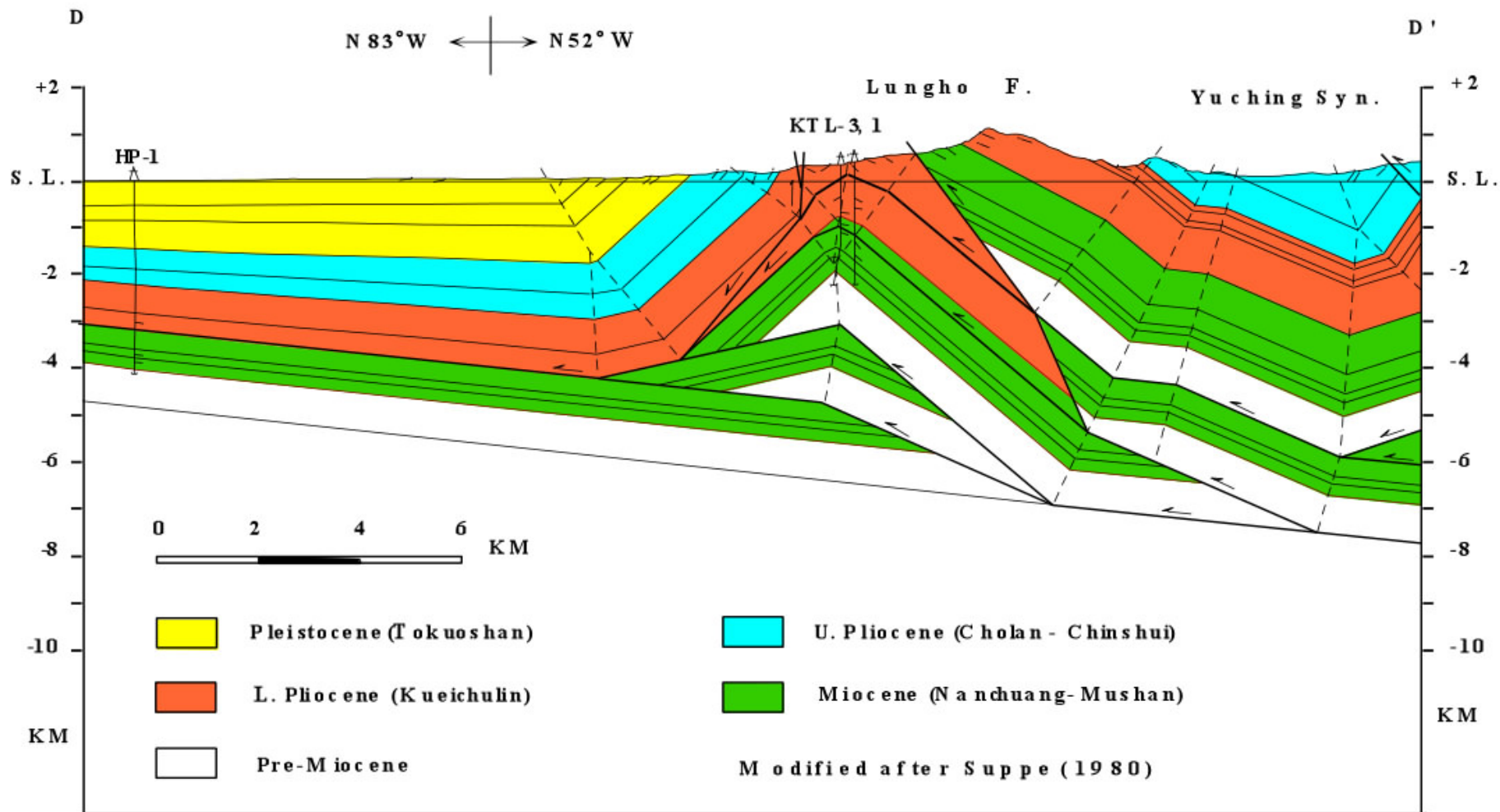
Stratigraphic Separation Diagram

Stratigraphic separation diagram helps to identify the location of the detachments.

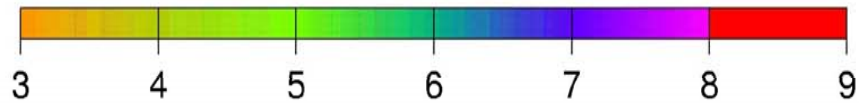
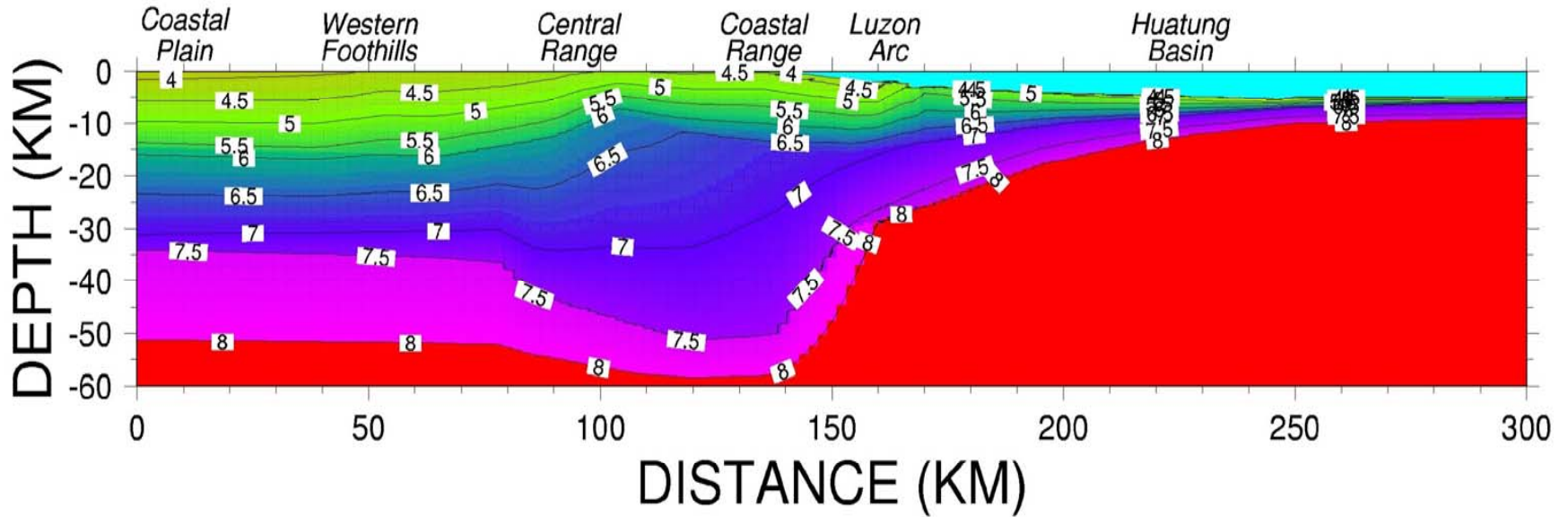


Fault-Fold geometry of a Decollement fault



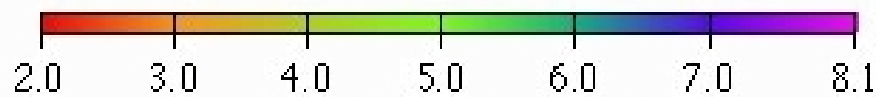
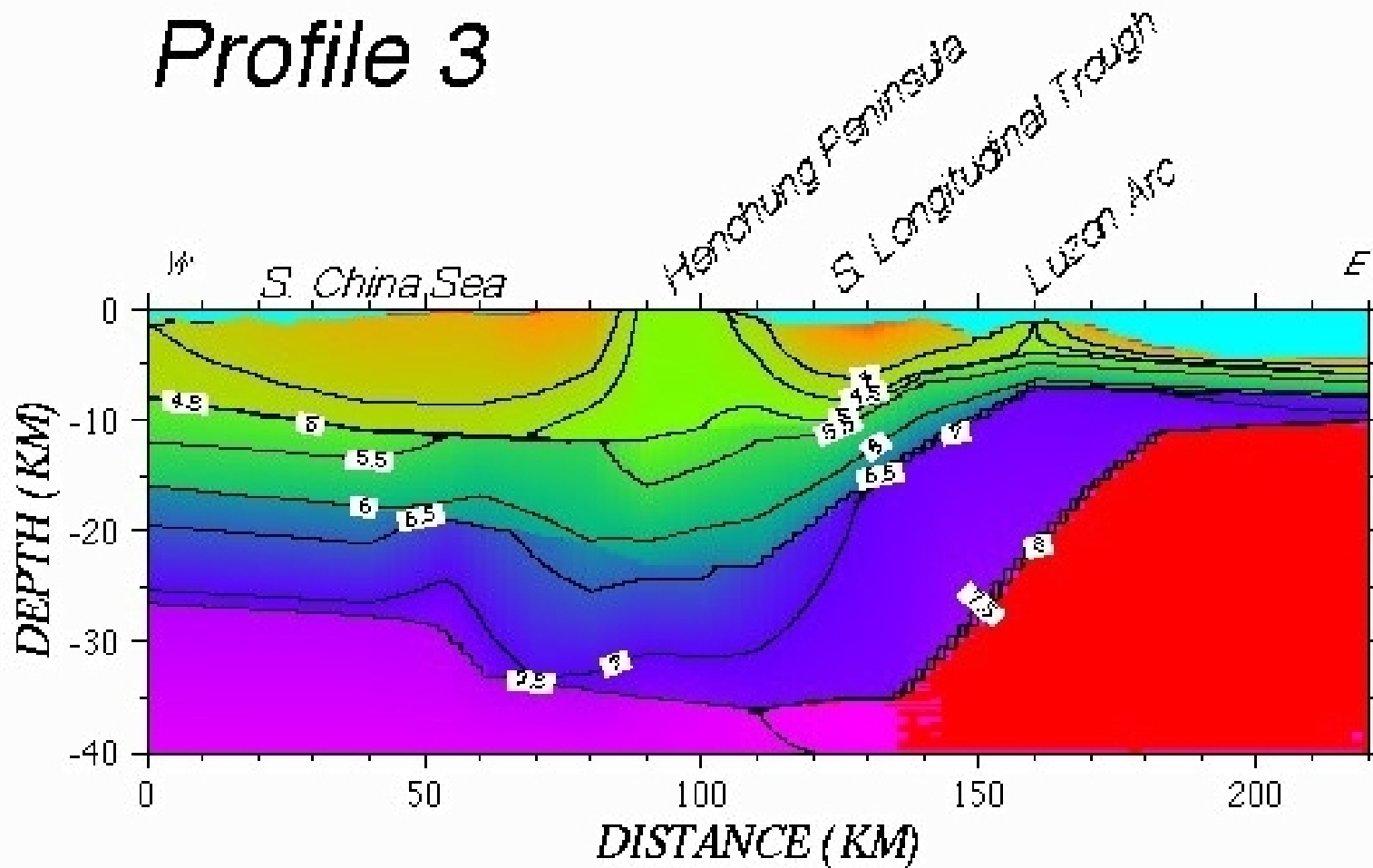


Southern Profile

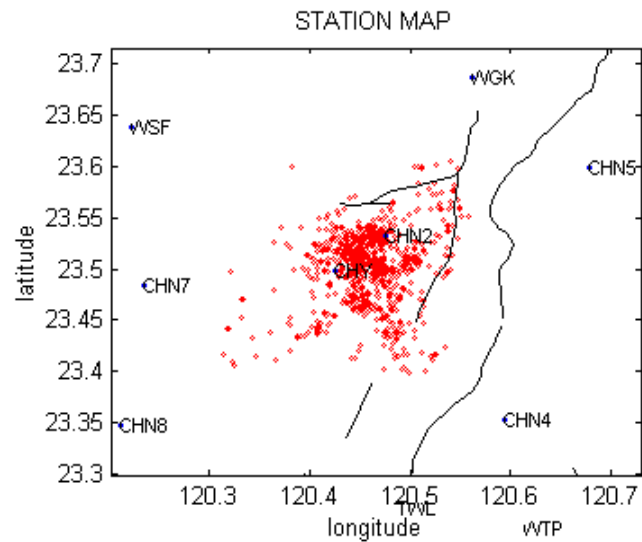


P-velocity

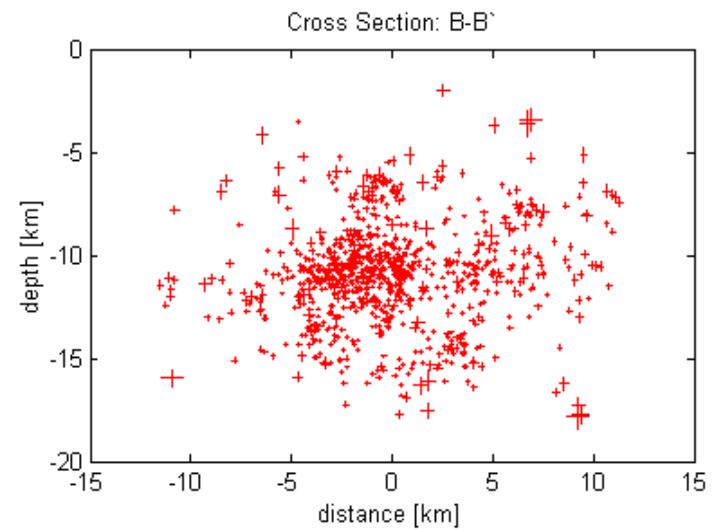
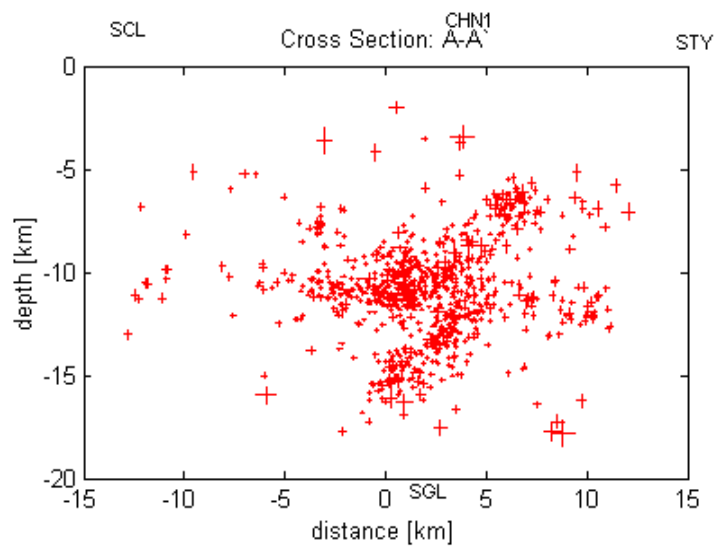
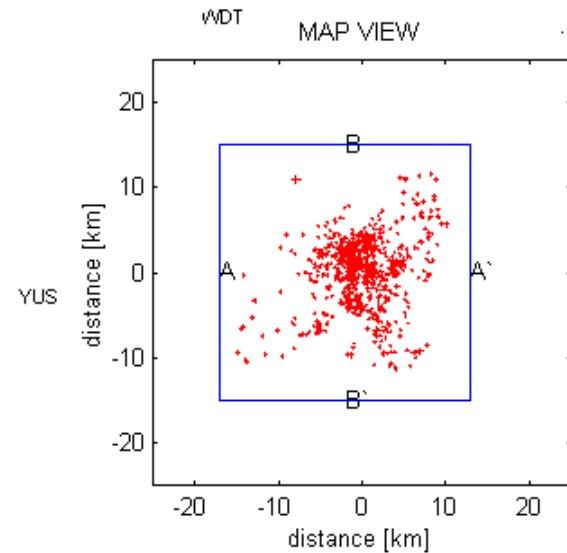
Profile 3



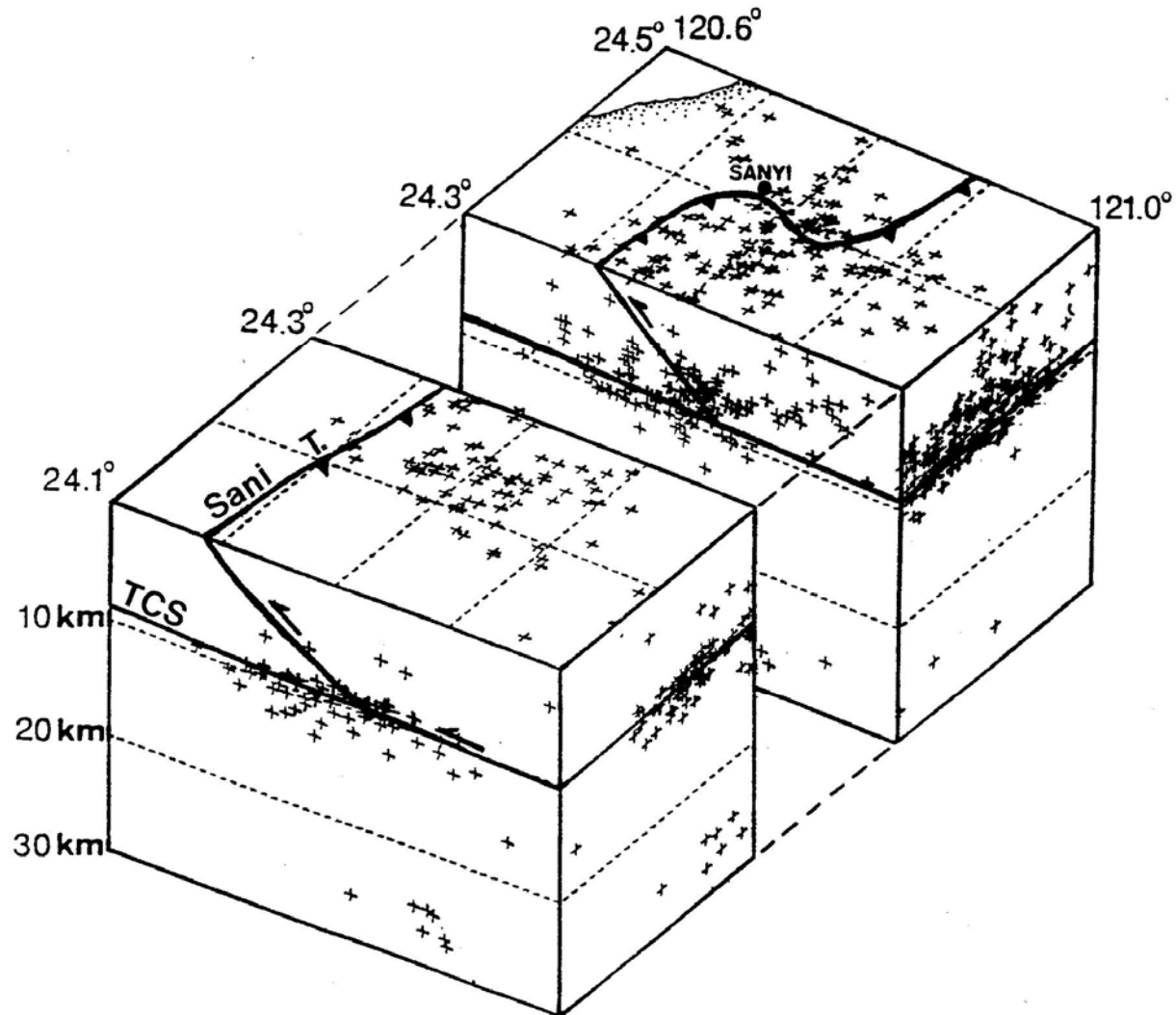
P-VELOCITY

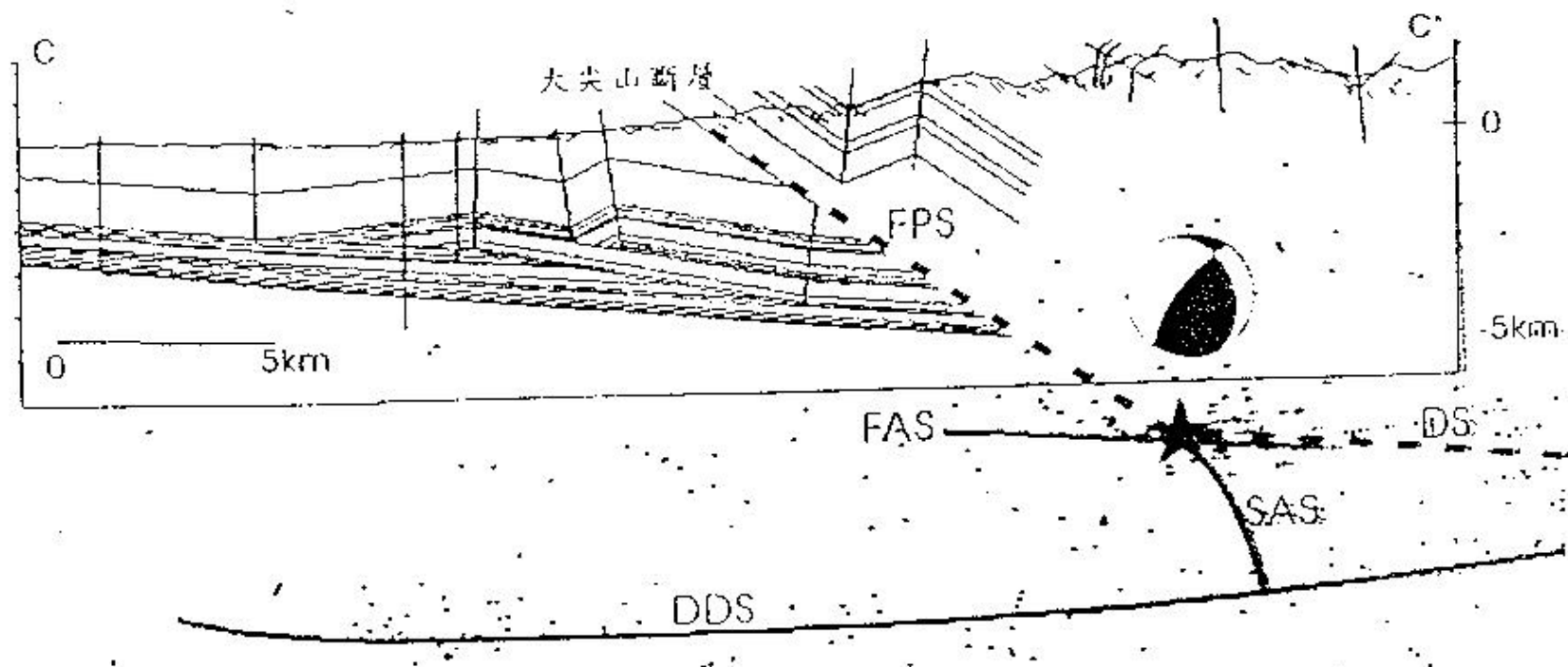


ALS

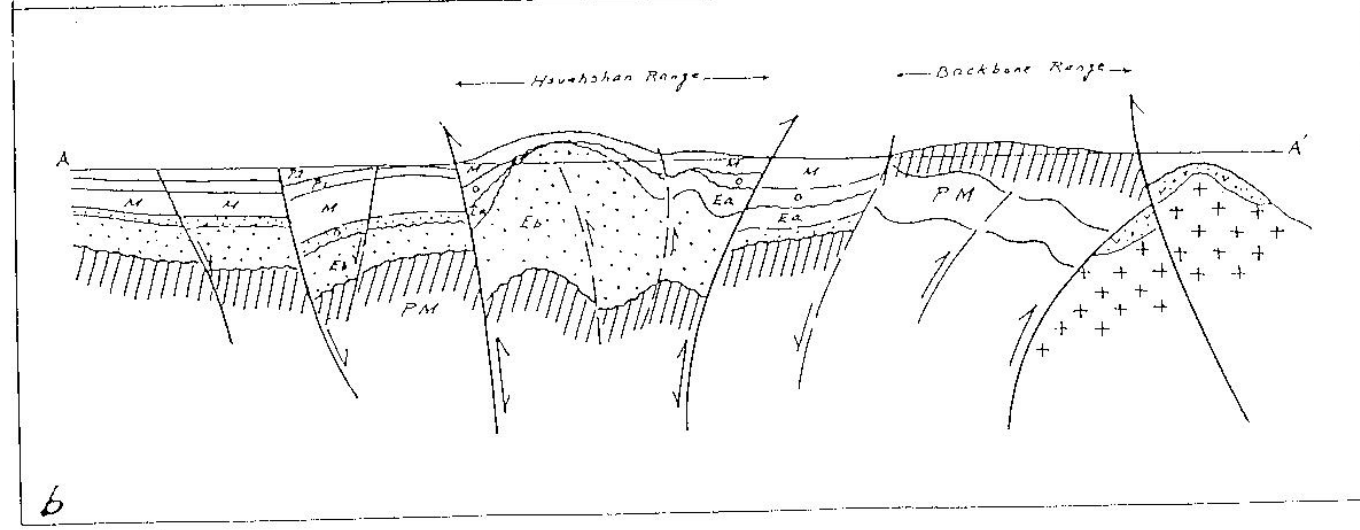
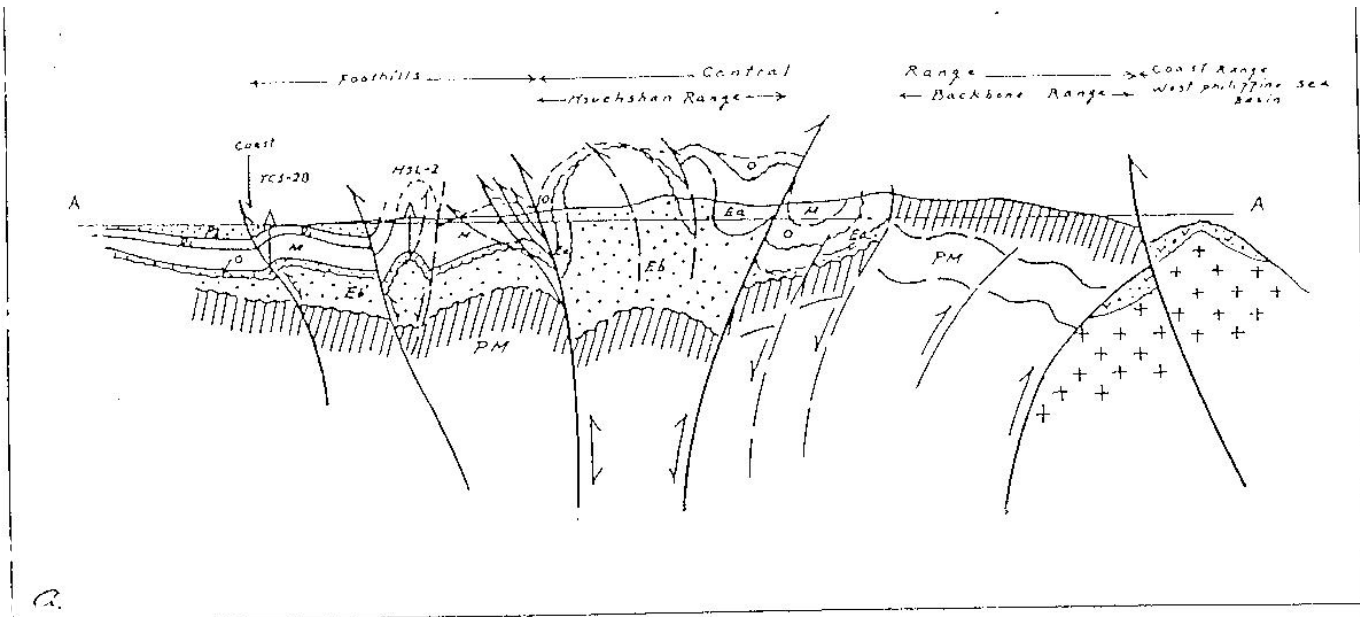


Earthquake indicated that Sani thrust is rooted between 8-10 km deep

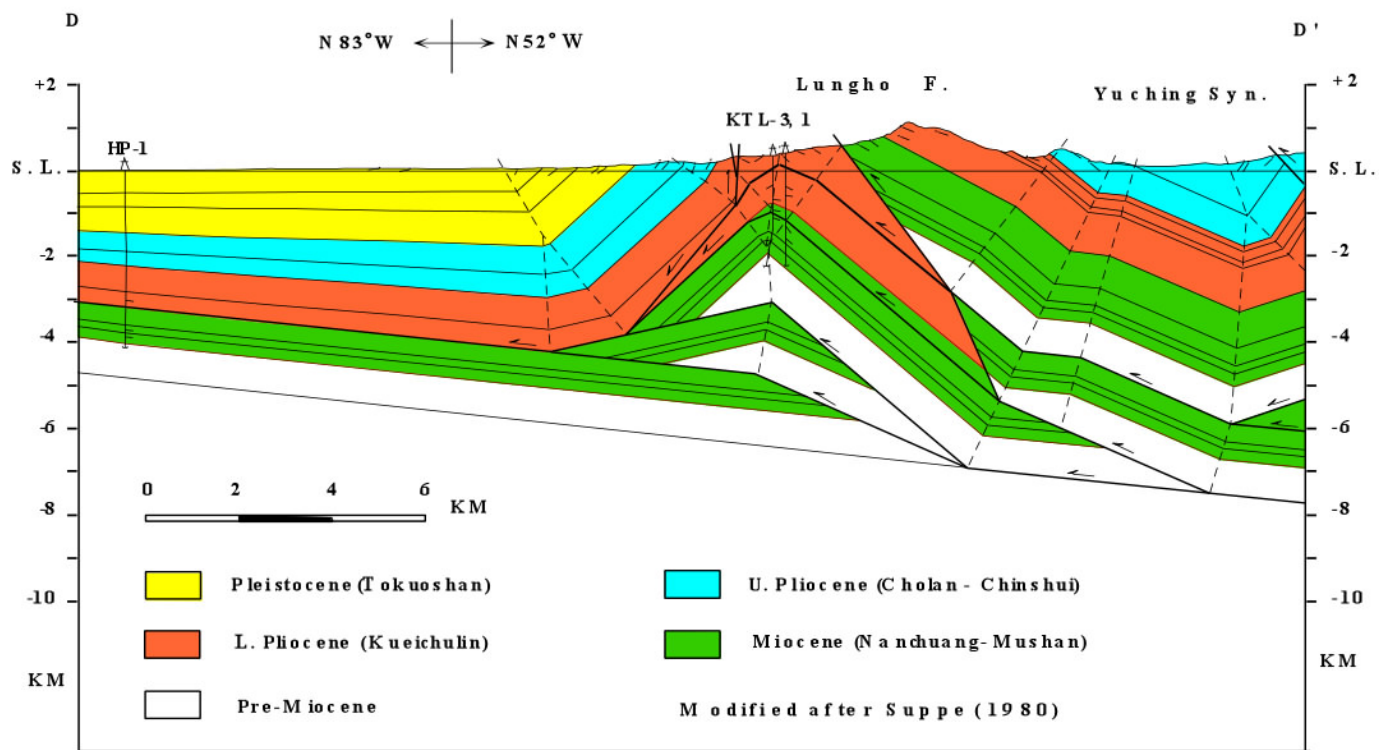
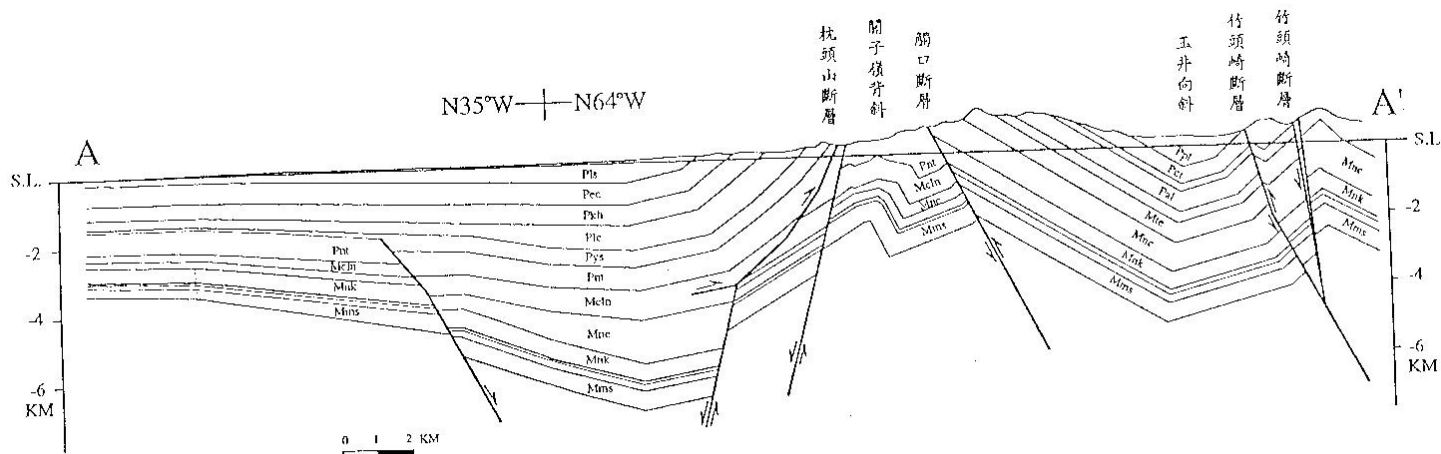




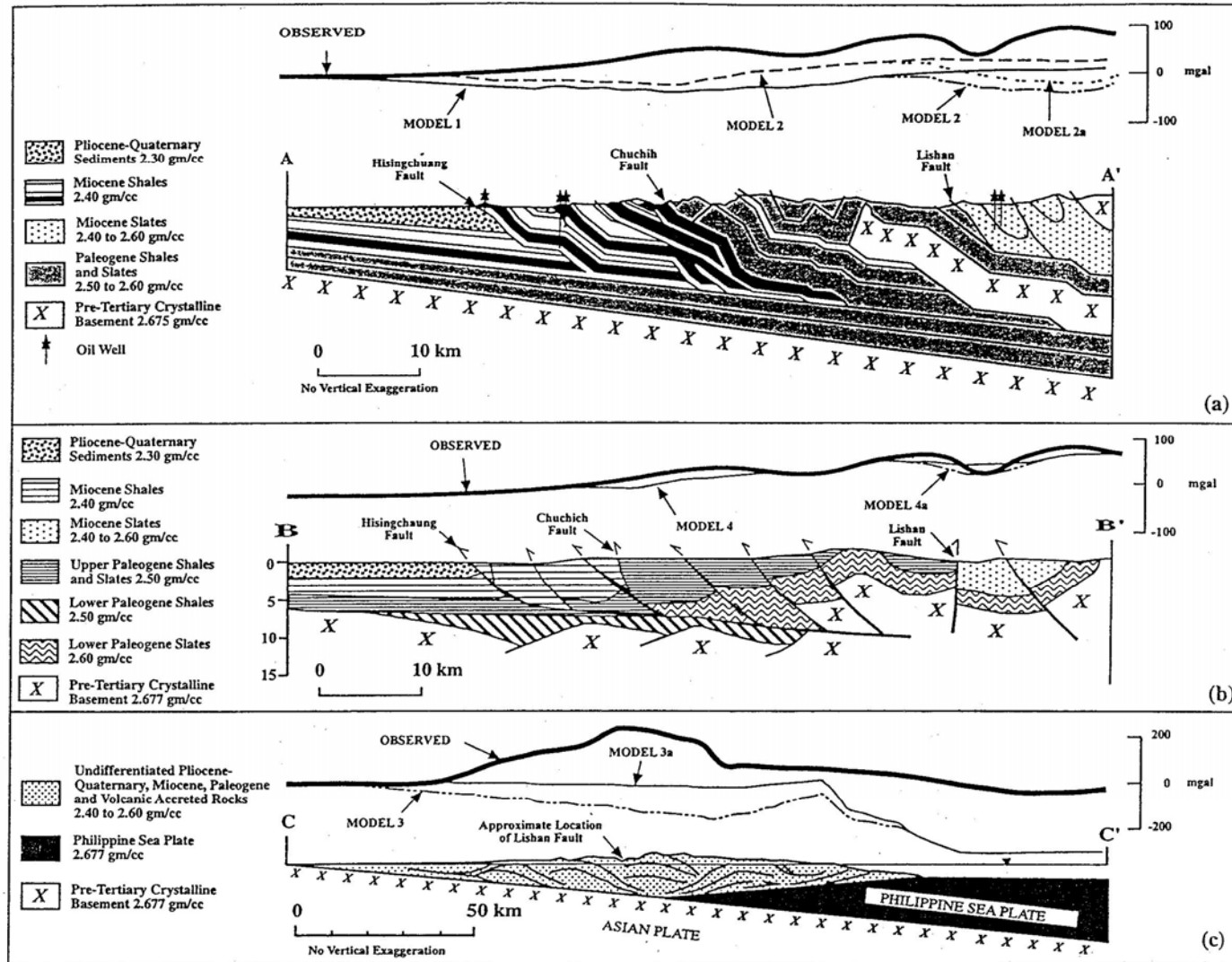
圖十九、瑞里地震與大尖山斷層剖面關係圖(羅博文, 2001)。沿 Suppe 平衡剖面截切之剖面圖，顯示震源機制解、大尖山斷層、瑞里餘震地震構造間之關係。星號為瑞里地震主震，黑點為剖面兩側地震投影，虛線為大尖山斷層截線，實線 FAS 和 SAS 為瑞里地震分布構造面截線，實線 DDS 為集集地震分布顯示之基底滑移面，海灘球為主震之斷層面解結果(高弘提供之 BATS solution)。



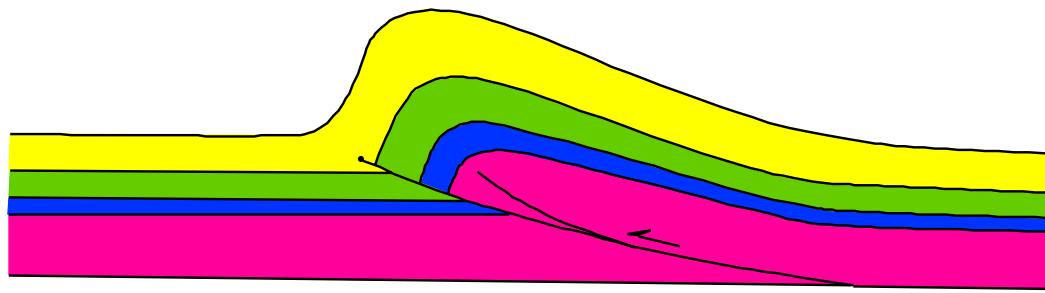
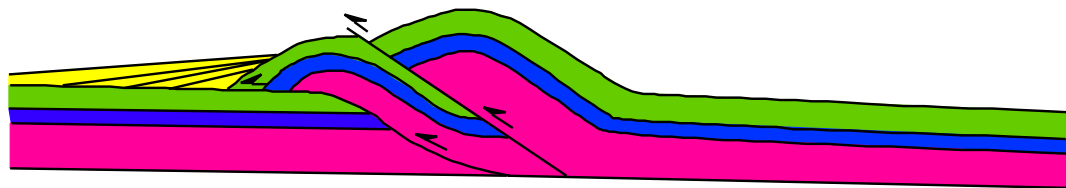
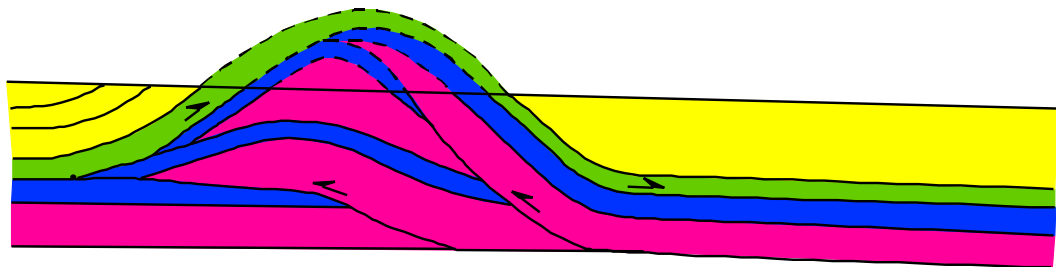
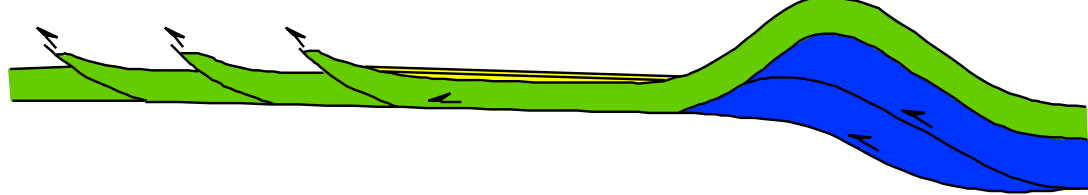
Thick-skinned
(above) and
thin-skinned
(below)
interpretation
of the
structures near
the Kuanzulin
anticline



Gravity model shows that the material underneath Central Range is not compensated by thin-skinned tectonics



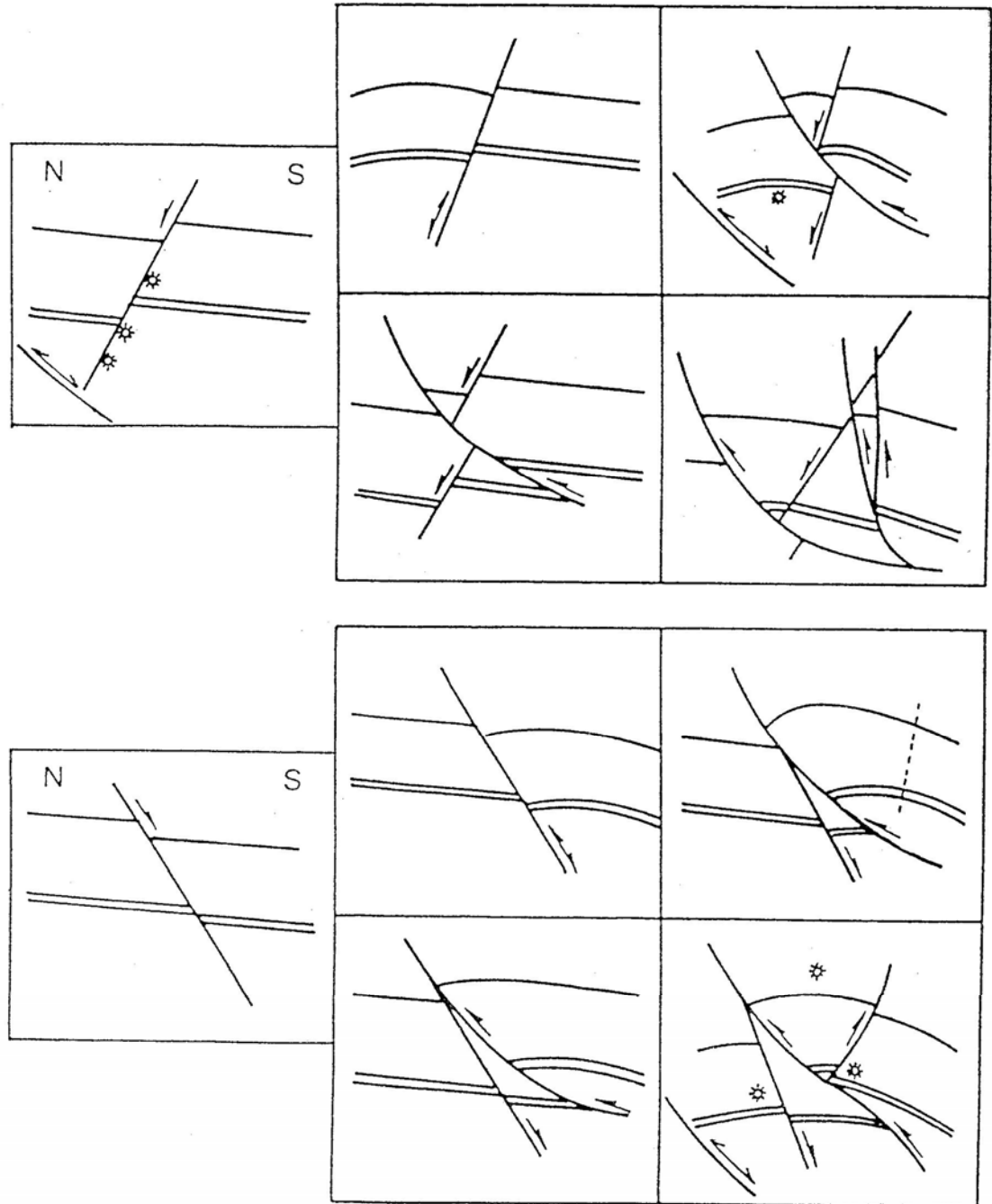
造山帶
前緣的
褶皺-斷
層構造



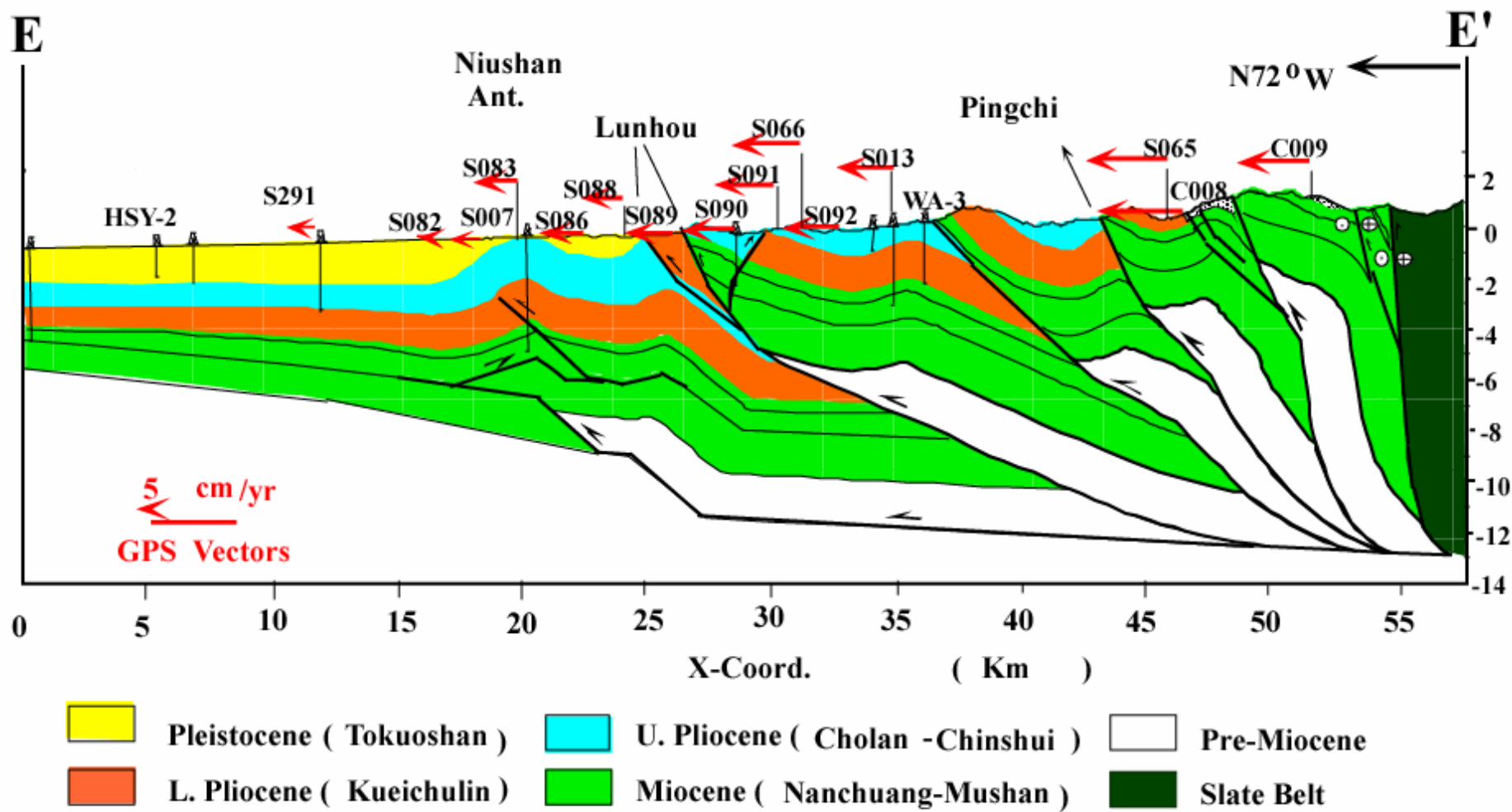
Evidence of Reactivation on the Pre-existing Normal Fault

- Abrupt change of facies and stratigraphic thickness across major thrust (reverse) faults
- High-angle dipping reverse faults at depth (>10 km)
- Change of stratigraphic separation from pre-extensional units to syn-extensional units
- The presence of high pore pressure zones between the Miocene Nanchuang and and Pliocene Niaotsui Formations.

Noraml faults
reactivate as
reverse faults or
cut by later thrust
faults in western
offshore Taiwan
(star is the pay-
zone of gas
reservoir)

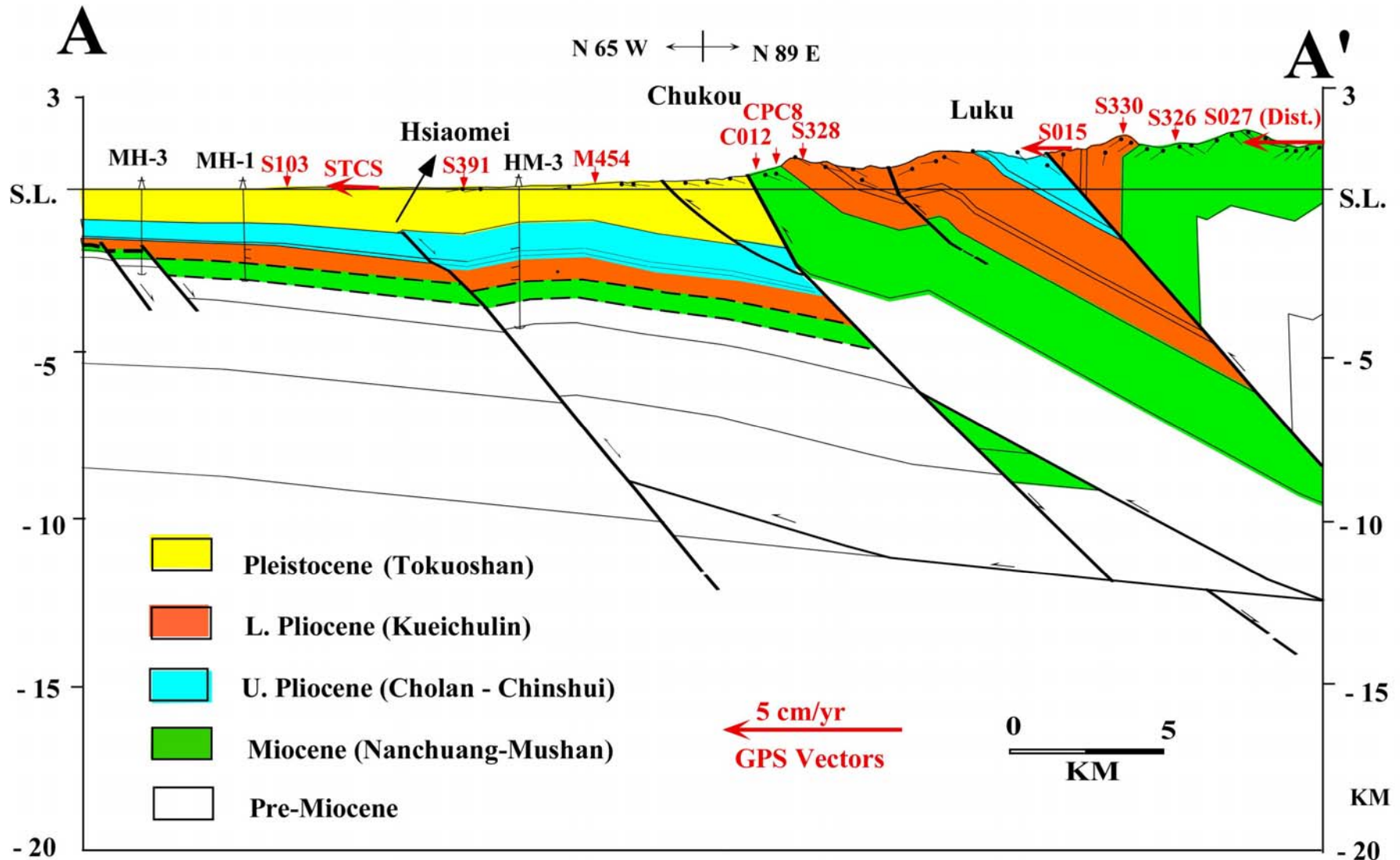


Gradual change of stratigraphic thickness (green color) across major thrust faults



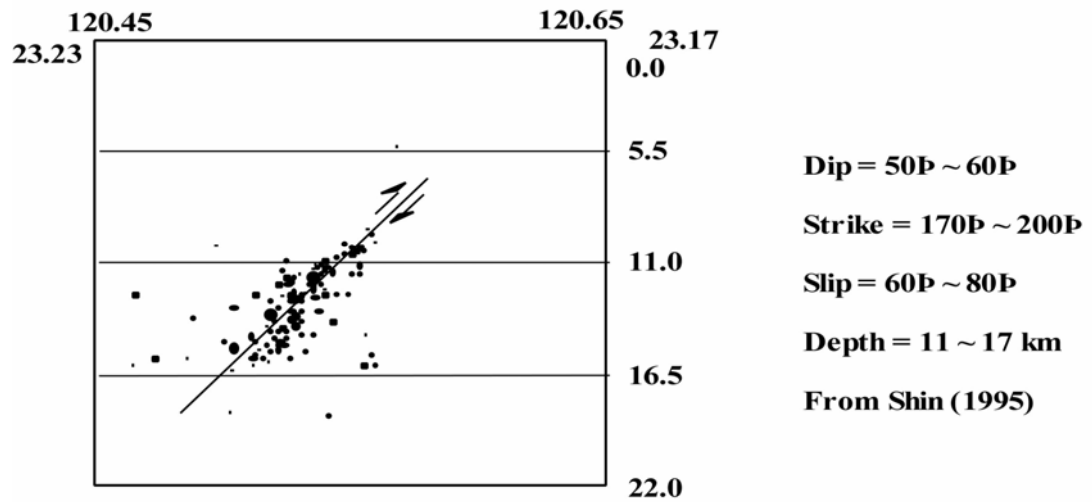
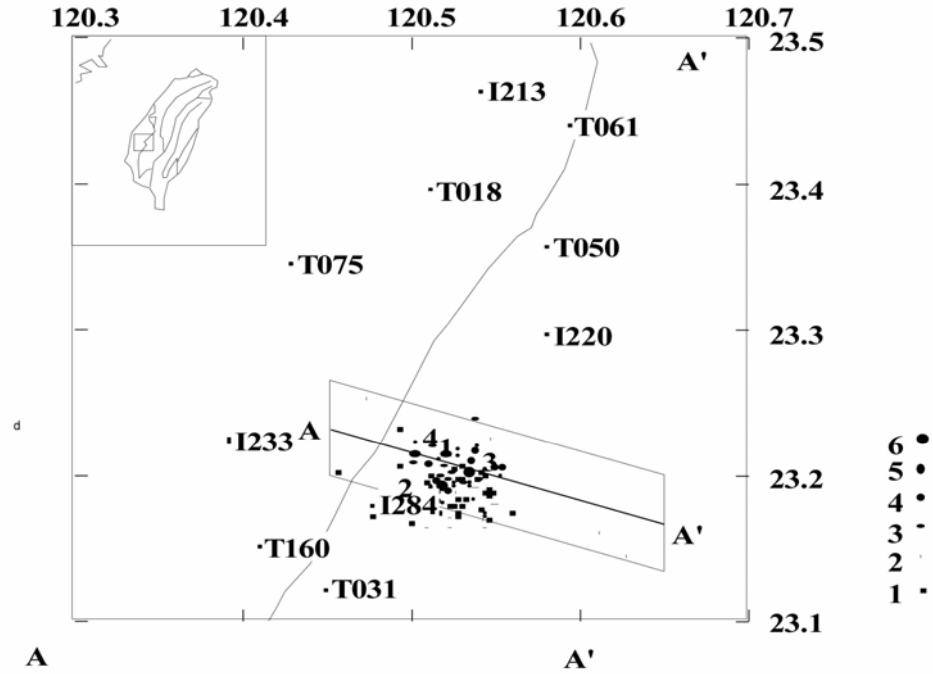
圖十七 E-E' 剖面及投影至剖面GPS測站之水平速度

Abrupt change of formation thickness (green color) across the Chukou fault, and high fluid pressure helps to reactivate at shallow part of the pre-existing normal fault



High-angle
reverse fault at
depth (Tapu
earthquake fault)

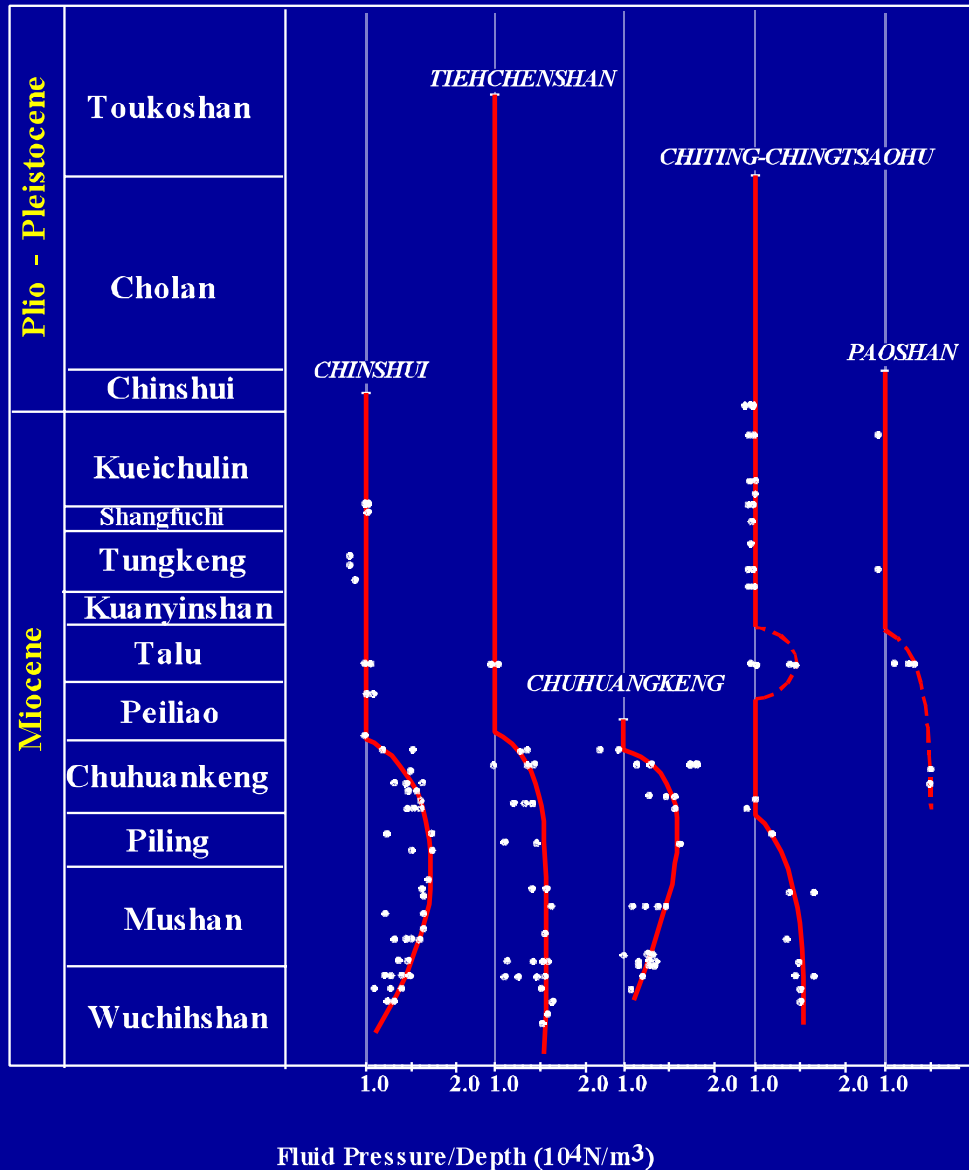
Tapu Earthquake Sequence



Fluid Pressure / Depth ratio and Stratigraphic Horizon in North-central Taiwan

Abnormal Fluid pressure encountered in wells drilled in the Foothills belt of Western Taiwan

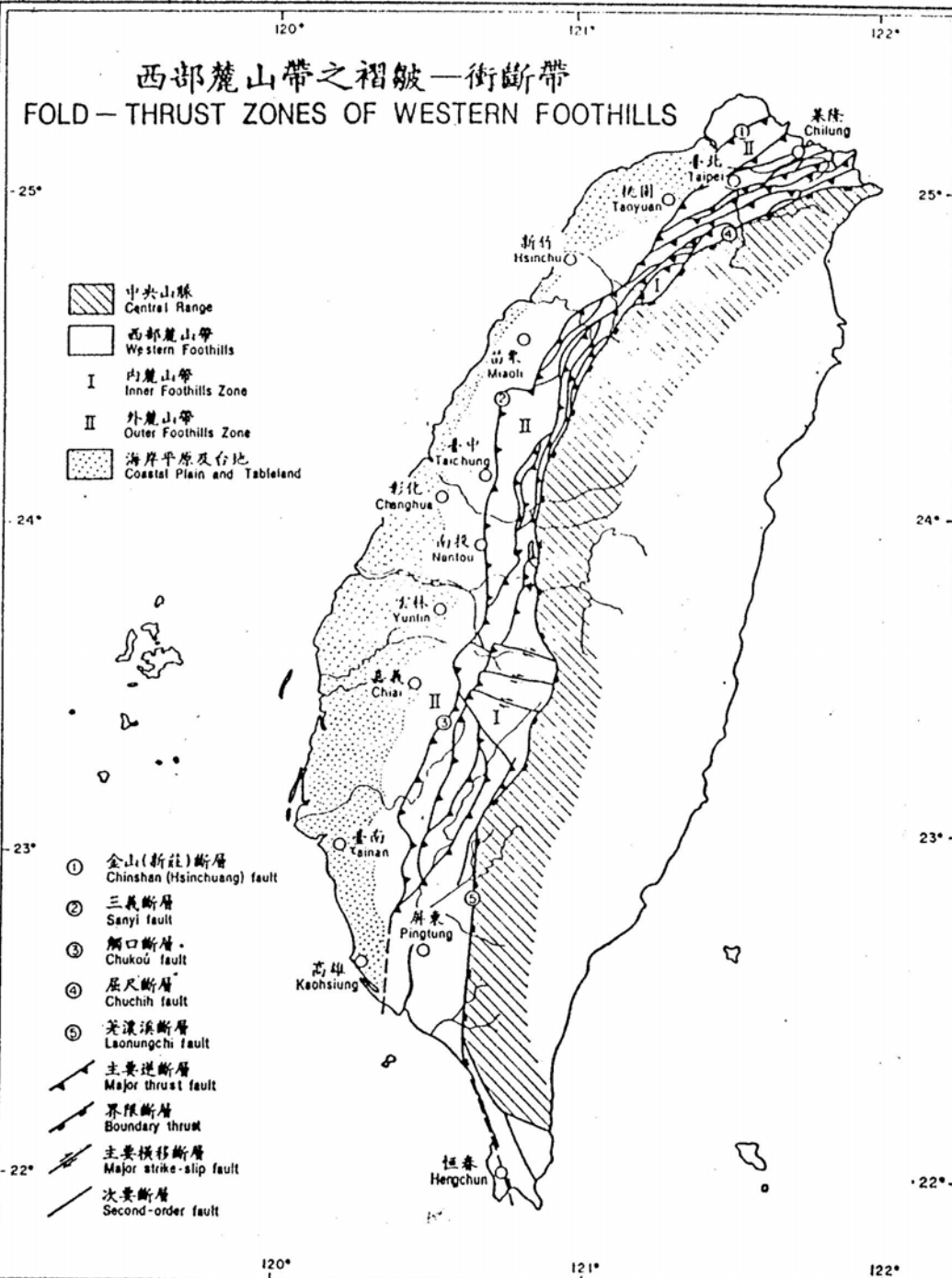
$$\lambda = P_f/P_r \sim 0.7$$



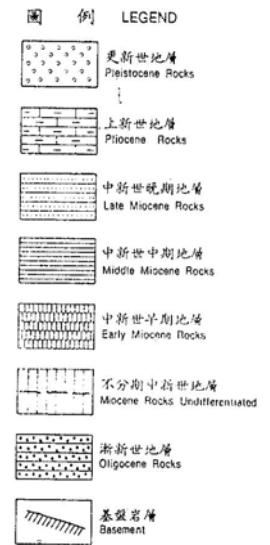
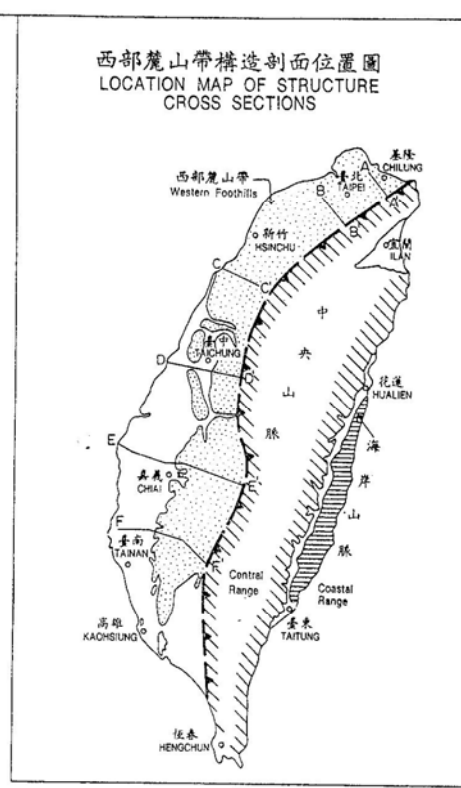
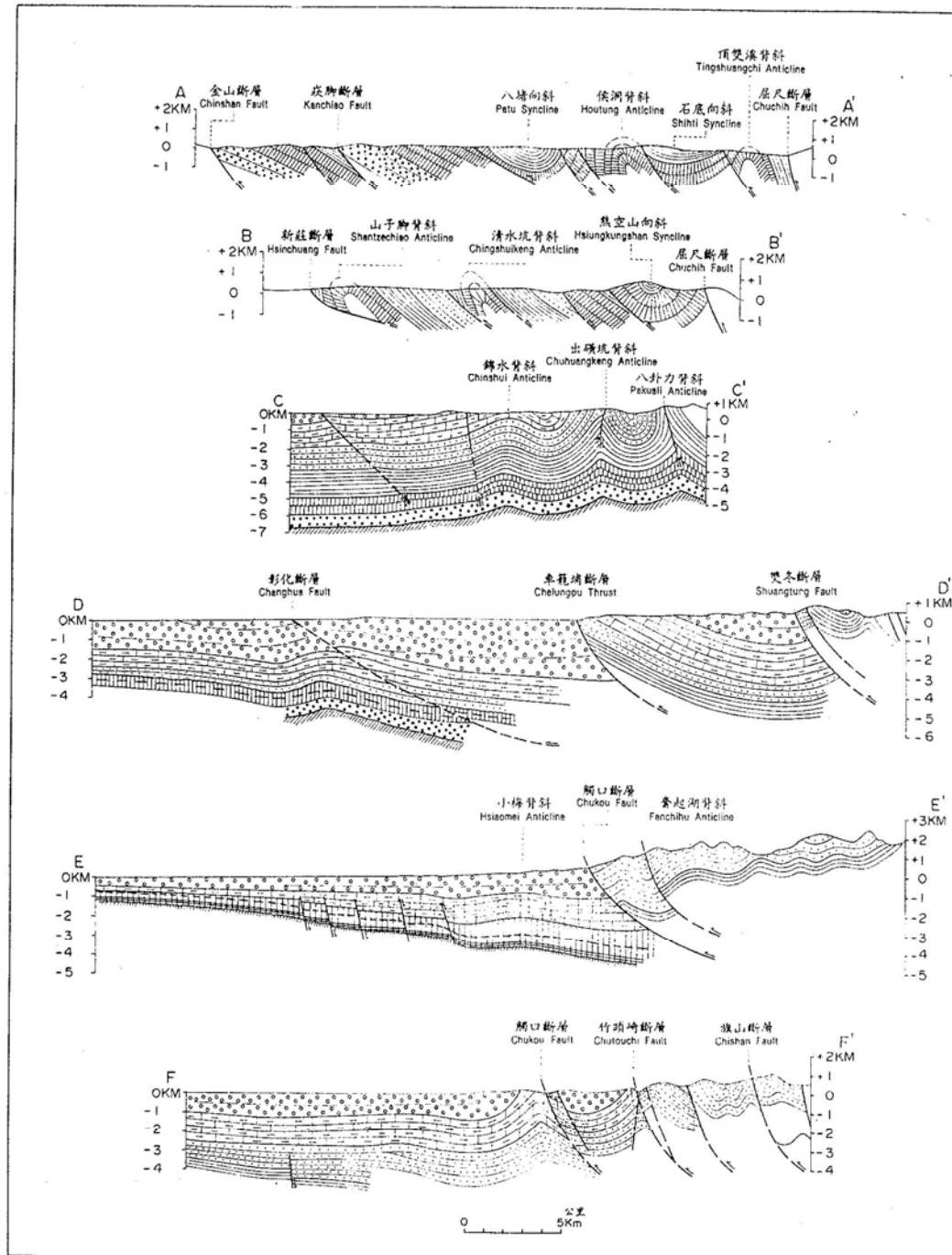
逆衝斷片的移動機制

- 逆衝斷層作用在力學的矛盾
- 力學矛盾的解答
 - 超正常流體液壓 (Hubbert and Ruby, 1959)
 - 斷層岩石呈流體或塑性變形 (Kehle, 1970)
 - 重力擴散(Elliot, 1976)
 - 重力下滑 (Hubbert and Ruby, 1959)
 - 三角楔形體
 - 塑性流動楔形 (Chapple, 1978; Stockmal, 1983)
 - 脆性摩擦楔形 (Davis et al., 1983)

西部麓山帶之褶皺—衝斷帶
 FOLD-THRUST ZONES OF WESTERN FOOTHILLS

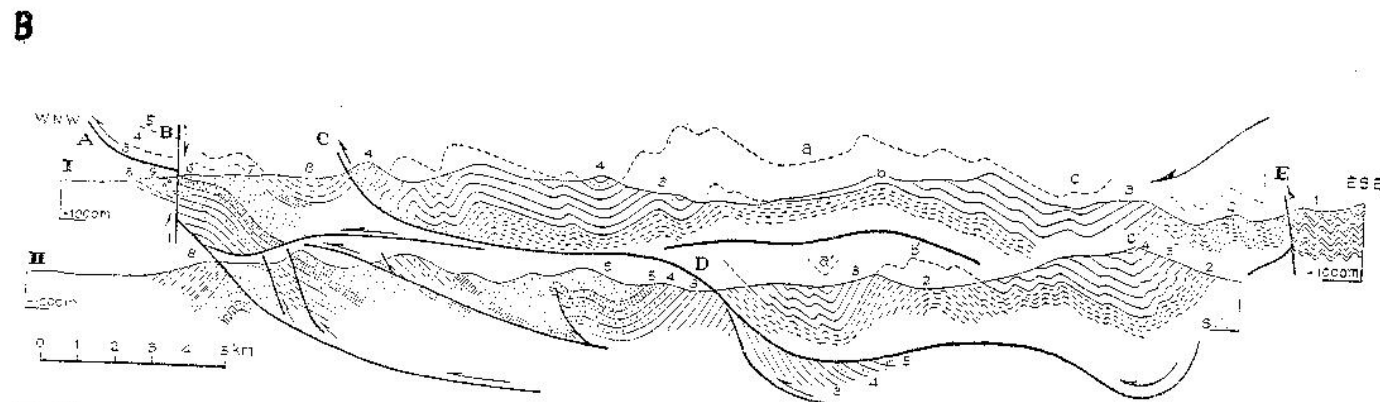
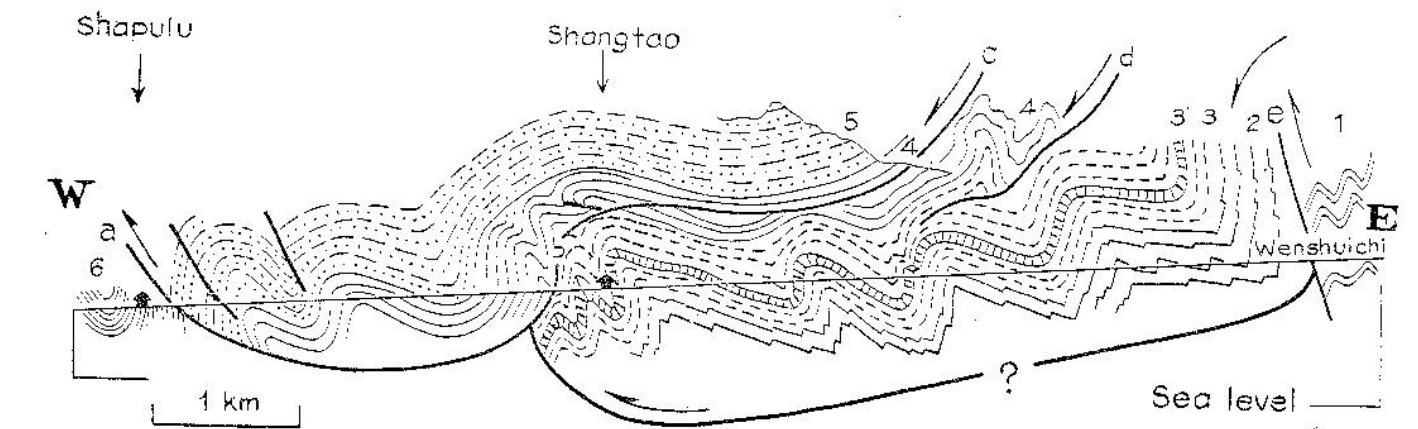


Fold-thrust Belt of Western Taiwan



圖七、西部麓山帶地質構造剖面圖(依據何春蓀,1974 及周瑞燾,楊健一,1986)。

Gravity sliding of the Alishan Nappe propose by Biq (1969, 1972)



圖二十一、台灣汶水溪(圖 A)及阿里山(圖 B)逆衝斷層之構造剖面，指示重力俯衝運動之作用(依據畢慶昌,1969；1972)。

Coulomb-Frictional wedge Model

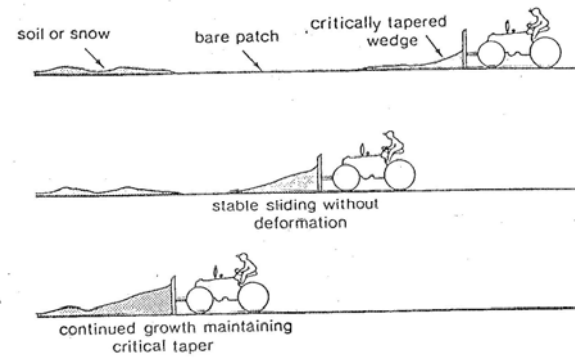
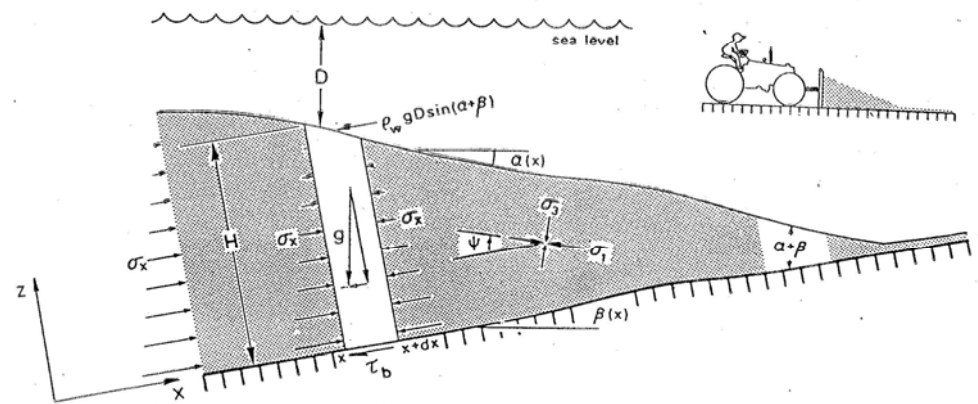


Figure 1. The wedge of soil or snow in front of a moving bulldozer grows self-similarly as freshly plowed material is encountered at the toe. The critical taper is the shape that is just strong enough to be slid over a bare patch without steepening or deforming.



$$\alpha + \beta = \frac{(1 - \lambda_b) \mu_b + (1 - \rho_w / \rho) \beta}{(1 - \rho_w / \rho) + (1 - \lambda) K}$$

K : dimensionless quantity

For Sandbox $\lambda = 0, \rho_w = 0$

Key Parameters:

$$\alpha + \beta = \frac{\mu_b + \beta}{1 + K}$$

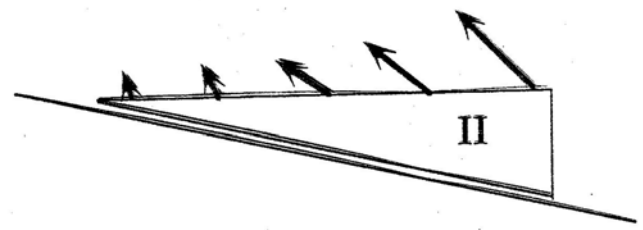
- Erosion
- Strength of basal units (μ_b)
- Rock strength (μ)
- Sedimentation and Faulting (Isostasy)

Surface motion of various Wedge States

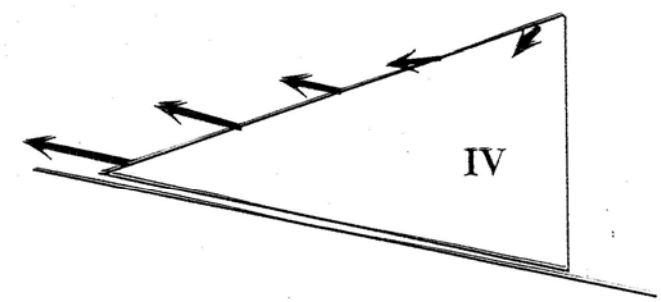
(A) Critical Wedge



(B) Subcritical Wedge



(C) Supercritical Wedge



圖二十二、增積楔型體在不同的發育狀態地表可能的運動方式：(A)臨界, (B)次臨界, (C)超臨界狀態楔形體 (依據 Wiltschko et al., 2000)。